Liquid-Metal-Wetted Rolling-Contact Current Collectors

by

Che Keung Ma

Submitted in partial fulfillment
of the requirements for the degree
of Master of Applied Science

Department of Electrical Engineering,
Faculty of Science and Engineering,
University of Ottawa,
Ottawa, Canada.

1973

Abstract

A liquid-metal-wetted rolling-contact current collector which should be particularly suitable for the homopolar machines, was investigated. The rolling contact was obtained through the use of steel balls held in races whose surfaces were wetted by Wood's Metal.

Three fundamental aspects of the current collector were analysed: a) the magnitude of the contact area of a ball pressing against a plane surface, b) the existence and magnitude of the repulsive and the constrictive electrodynamic forces on contacts, and c) the relation between the voltage and the temperature of a symmetric contact.

The electrical properties of stationary contacts between two bare brass surfaces, and then between two brass surfaces coated with Wood's Metal, were experimentally investigated. Then the voltage-current characteristics of the rolling contacts between surfaces, both bare and coated were investigated. Finally, rolling-contact current collectors with bare surfaces, and also with surfaces wetted heavily with liquid Wood's Metal, carrying currents up to 250 A, were investigated.

The results for the wetted case showed that the voltage drop per contact interface was less than 0.05 V, which compares favourably with about 0.5 V voltage drop for the carbon brush. This indicated that further research on this type of current collector seems to be warranted.

Acknowledgments

I am indebted to Prof. O. Celinski for introducing me to the subject of current collection for the homopolar motor, and for supervising my work on this thesis.

I thank Dr R. E. Bedford of the National Research Council of Canada for his support of my post-graduate work, and for his editorial comments on this thesis.

I also thank the Department of Electrical Engineering at the University of Ottawa, and the Division of Physics at NRC for affording me the opportunity of pursuing post-graduate studies.

Finally, I would like to thank my wife, Rose, for her constant encouragement.

Table of contents

Page

List of Tables

List of Figures

I. Introduction

1.1. Air Pollution due to Automobile Emissions

Pollution of the natural environment is causing growing concern among the public, industries, govenrments, and nations. Evidences for this concern are many: discussions (occasionally occurred in daily conversations) among individuals on the disposal of bottles and cans; efforts by industries to produce, for example, low-emission automobiles and phosphate-free detergents; recycling of used newsprint, currently being practised, for example, in Ottawa; "clean-up" of the Great Lakes to be jointly carried out by Canada and the United States; and the United Nations' conference on the human environment in Stockholm (June, 1972).

Our natural environment can be broadly divided into three sectors: air, water, and soil. The pollution of air comes from a variety of sources, of which the automobile is a major one in urban areas. It is claimed (1) that an average automobile, probably without anti-pollution devices, emits each year 770 kg of carbon monoxide, 230 kg of unburned hydrocarbons, 40 kg of oxides of nitrogen, and 2 to 5 kg of particulate matter. In the United States emissions from automobiles account for about 50% of the air pollution (2). The seriousness of air pollution by automobiles is evident from the stringent U. S. federal regulations on automobile emissions applied to models of 1968 and later years. In Canada the same concern is evident from the regulations which first came into effect on January 1, 1971, and from the "International Conference on Automobile Pollution" held in Toronto during June 26-28, 1972.

1.2. Solutions to Automobile Pollution

An obvious solution to the problem of pollution by automobiles is to ban or restrict their use. However, a complete ban is unacceptable because they are an essential means of transportation. Even a partial restriction of their use would cause a serious disruption in industries and society. Although the evolution of a new transportation system in the form of modules running on roadbeds and controlled by automatic guidance systems is foreseeable (3), there is as yet no other alternatives capable of replacing the automobile transportation system. Consequently the only acceptable solution to the problem for the immediate future is through designing non-polluting automobiles.

The emissions from the present-day automobile are mainly from three sources: crankcase, exhaust, and fuel system. The chief pollutants in automobile emissions are lead, unburned hydrocarbons, carbon monoxide, and oxides of nitrogen. It is technologically feasible to reduce these pollutants to within acceptable limits.* Lead emission can be eliminated by the use of unleaded gasoline. Crankcase emissions are reduced by using a crankcase ventilating system. The fuel vapours from the fuel system can be prevented from escaping into the atmosphere by directing them to a charcoal filter for absorption and also to the intake manifold for combustion. The pollutants in the exhaust can be significantly reduced by detailed improvements in the designs of the carburetor, intake manifold, and combustion chamber to achieve near-complete combustion,

---

* Two Japanese firms recently had claimed, based on performances of their test automobiles, that they could produce, on a mass scale, automobiles to meet the anticipating 1975 U. S. anti-pollution requirements. One firm equipped their test automobile with a rotary engine, while the other, with a modified version of the conventional internal combustion engine using stratified charge.

and by the purification of the combustion product. Purification is achieved by injecting fresh air into the exhaust manifold to oxidize the unburned hydrocarbons, and by passing the exhaust gas through a catalytic converter (1,4) to eliminate certain noxious compounds. However, the addition of emission control devices increases not only the capital cost but also the maintenance costs of the automobile, therefore making it a greater financial burden to the owner. Moreover, the manufacture of these devices and their later disposal will further aggravate the problem of pollution.

Some commercial firms (5) have been successful in modifying the internal combustion engine to operate on cleaner fuels such as butane or propane, which give a much cleaner exhaust. However, the production of such liquid petroleum gases is sufficient to satisfy only 5 to 10% of the automobile demand (1). Consequently, using them as fuels for the internal combustion engine is not likely to solve the pollution problem.

It seems necessary to look for alternatives to the internal combustion engine. Several are already available: the Stirling engine* (6), the steam engine, the gas turbine, and the electric motor, but it is difficult to predict if any of these will become acceptable. Nevertheless, some of their inherent characteristics and relative merits relevant to the pollution problem are known for certain.

- -

* The Stirling engine was invented by a Scottish priest, Robert Stirling, in 1816. Similar to the steam engine, it is an external combustion engine. The working fluid of the Stirling engine is usually helium, and obtains its heat energy by conduction from a heater outside the cylinder. Now at high temperature and pressure, it is driven into the cylinder, and then allowed to expand, giving a power stroke. It is subsequently returned to a cooler and eventually to the heater via a regenerator for another cycle.

In the Stirling engine, the steam engine, and the gas turbine, heat is supplied to the working fluid which then drives some moving parts to do mechanical work. In theory the heat can be obtained directly from a non-polluting source such as the sun; in practice, however, it must come from the burning of fossil fuels. In contrast to the intermittent explosions in the internal combustion engine, the combustion in all of these three engines is continuous, and hence can be made nearly complete by feeding excess air into the combustion chamber. The Stirling engine is distinctive from the steam engine and the gas turbine in that its working fluid operates in a closed system and does not have to be discharged to the atmosphere at the end of a working cycle.

The familiar electric motor is often noted for its being relatively silent, reliable, maintenance-free, and vibration-free. In addition, it is fumeless and thus virtually non-polluting. Its use for automobile propulsion would shift the source of pollution from hundreds of millions of automobiles to a small number of power-generating plants, which supply energy for operating the electric automobile. This shift is of importance, because the pollution problem would become much easier to solve. For example, locating these plants in remote areas would isolate their pollutants from most of the population. Further importance would accrue through the use of non-polluting hydro-electric power rather than nuclear power (discharging nuclear wastes) or fossil-fueled power (producing harmful combustion products). Canada has an abundant hydro-electric supply and is, in this respect, in a favourable position for the use of electric automobiles.

The electric automobile as an alternative to its internal combustion counterpart has often been discussed (2,3,7,8,9), and seriously assessed (10,11). It will suffice to say that it is technologically feasible to build an electric automobile comparable to the internal combustion one in acceleration and top speed, but, as yet, considerably inferior in driving range. The range of a battery-powered automobile between recharges is only about 50 miles. Fortunately, fuel cells show promise of extending this range.

1.3. Electric Motors for Automobile Propulsion

Batteries and, recently, fuel cells as power sources in electric automobiles (10,11,12) are dc. Therefore it is logical to use dc motors for automobile propulsion, and, historically, they were used in electric automobiles. With the advent of modern, low-loss, low-cost, solid-state devices, it has become feasible to convert dc into ac, and thus ac motors can also be used.

In general, dc motors are of three types: series, shunt, and compound. The torque-speed characteristic of the first satisfies the requirements of automobile propulsion much better than the latter two (Fig. 1). Among the various ac motors, the induction motor is more suitable for automobile propulsion because of its simplicity, ruggedness, and reasonably good starting torque. Therefore, the dc series motor and the ac induction motor have attracted the most serious attention (13).

Generally speaking, speed control for the series motor is much simpler than for the induction motor. When design simplicity and overall cost are the main objectives, the series motor is preferred. However, its maximum speed is limited by the dynamic balance of the heavy wound rotor and the commutation of the armature current. In comparison, the induction motor, because of the inherent ruggedness of its rotor and the lack of commutation, can run at a much higher speed. Since higher speed implies higher power output, the rating of the induction motor is generally larger than that of the series motor of similar weight and size. Therefore, the induction motor is preferred when the requirement demands a motor of large power rating (more than 30 kW). Data for some typical motors of these two types are shown in Table I.

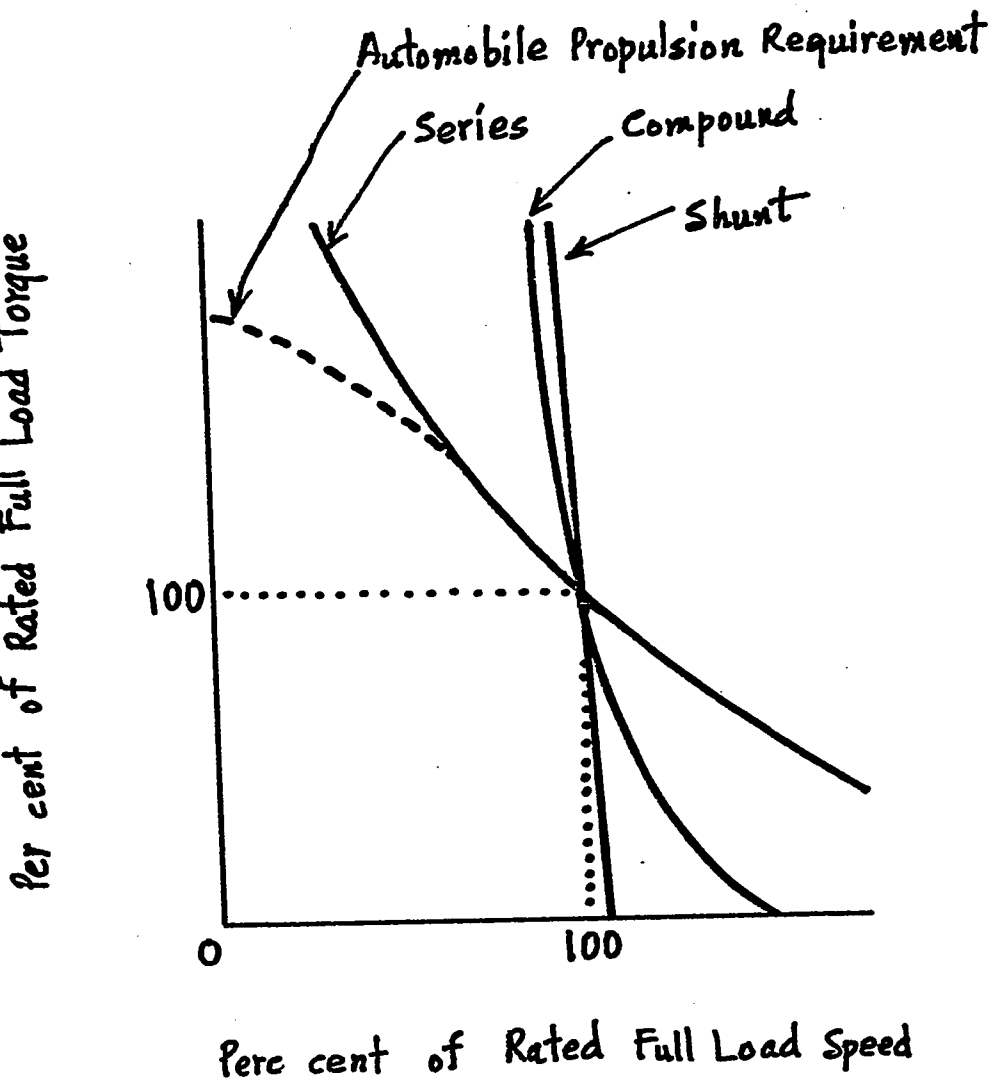

Fig. 1 : Torque-Speed Characteristics of d c Motors (37)

Table I

Examples of Motors for Electric Automobiles (13,14)

	dc series motor		3-phase ac induction motor
	a	b	
(continuous) power rating (kW)	8	30	67
speed (rpm)	3200	8000	13000
efficiency (%)	84	90	93
voltage (V)	72	120	530
cooling	open,fan cooled	blower ventilated	oil cooled
length (cm)	47	39	36
diameter (cm)	23	24	27
weight (kg)	75	73	59

There is another type of dc motor, the homopolar motor, which has been considered as a possible power plant for the electric automobile (8,15). Its advantages are many. It is inherently a low voltage machine, thereby eliminating the hazards of electric shock. This is important from the safety point-of-view. Furthermore, the low operating voltage reduces the overall leakage losses (insulation losses). Hysteresis and eddy current losses, and armature reaction, which are important considerations in some conventional motors, do not pose problems for the homopolar motor, because it operates in a different way. The rotor of the homopolar motor is usually a cylinder (hollow or solid), or a disc, as shown in Fig. 2. The inherent ruggedness of the rotor increases the reliability of this motor. The simple geometry of the stator favours the use of permanent magnets, instead of field windings, to provide the stator field. Thus, it is possible to construct a homopolar motor with no wires at all, and eliminate the failure due to the deterioration of wire insulation. The most distinctive feature of this dc motor, however, is that it does not require a commutator, but only a current collector. Thus, the problem of commutation is eliminated.

The road speed of an electric automobile must vary constantly to suit the driving situation and hence the motor that drives the vehicle should be highly responsive. The responsiveness of an electric motor can be indicated by what is commonly called the power rate,

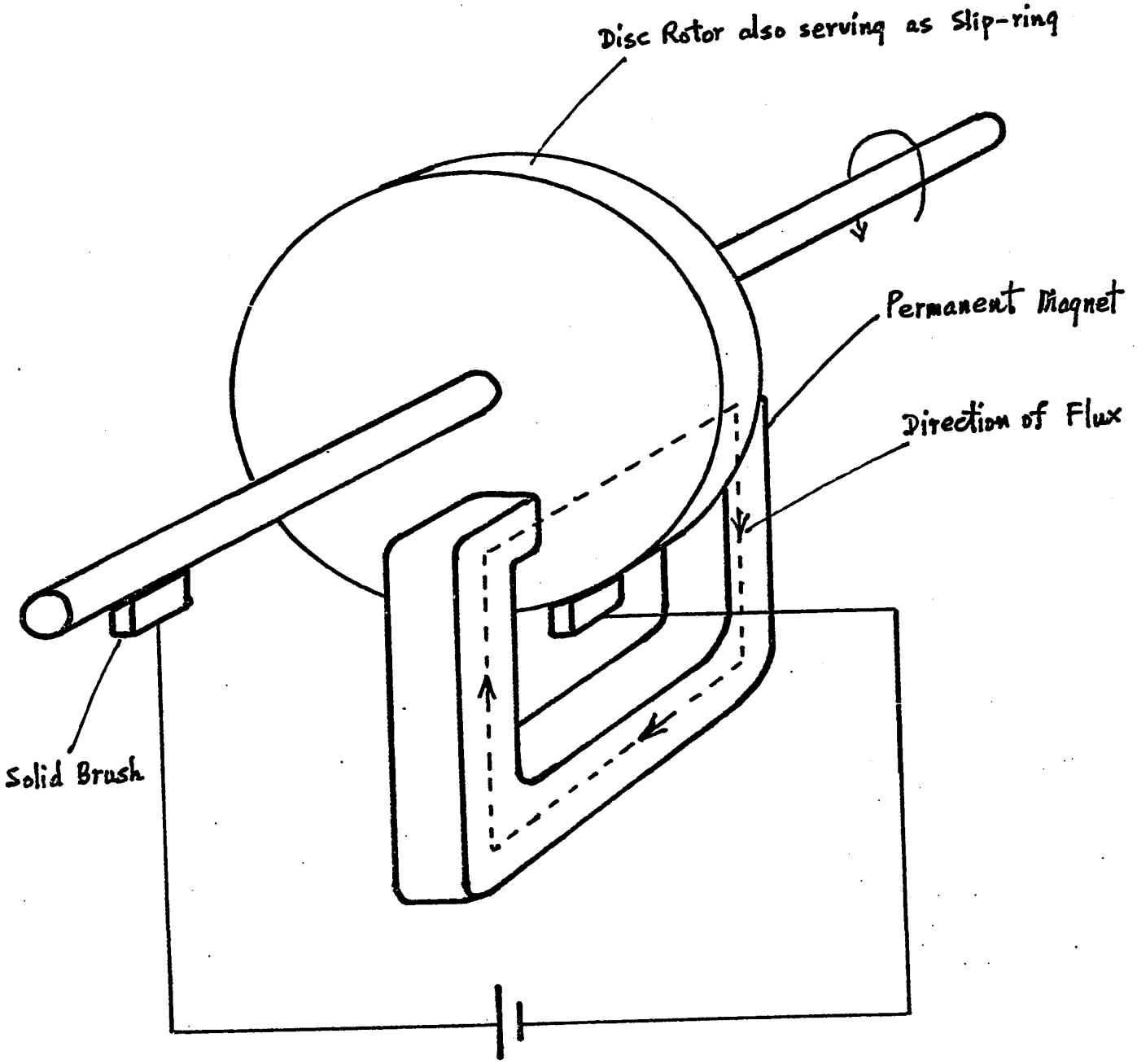

Fig. 2: A Simple Disc-Type Homopolar Motor

$\frac{T_{max}^2}{J}$ *, where T_{max} is the maximum torque, and J is the moment of inertia of the rotor. This is a measure of how quickly the motor can increase its output power under no external load. It has been estimated (16) that, on a basis of per kilogram of motor weight, the power rate of the homopolar motor is 85 kW/s. This is higher than that of the shell-type dc motor (60 kW/s, (17)).

The output power of a motor is given by the product of the torque and the angular speed. In practice, the maximum torque will be determined by the available magnetic field and by the maximum current that the rotor can safely carry. Further increase of output power without increasing the motor size must come from raising the maximum operating speed. In view of a related development for an electric motor (18), it is expected that the maximum speed of the homopolar motor will be in the region of 10 000 rpm. This high speed can be coped with, however, by incorporating a speed reduction unit such as an epicyclic gearbox (18).

---

* The time derivative of the output power of a motor is

$$\frac{dP}{dt} = \frac{d(T\omega)}{dt} = T\frac{d\omega}{dt} + \omega\frac{dT}{dt}$$

where P, t, and ω are the output power of the motor, time, and the angular velocity of the rotor. In practice, if the rotor current and the stator field are kept constant at their maximum values while the motor accelerates, the torque will remain constant at T_{max}. Therefore $\frac{dT}{dt}$ in the above expression becomes zero. In the absence of external load, $\frac{d\omega}{dt} = \frac{T_{max}}{J}$, where J is the moment of inertia of the rotor. Thus, $\frac{dP}{dt} = \frac{T_{max}^2}{J}$.

The homopolar motor, then, appears to be well-suited to automobile propulsion. We envisage an electric automobile of small to medium size, with a body of Fiberglas (Fibreglass) on a tubular frame. It will have a four-wheel-drive with a light-weight homopolar motor incorporated in each wheel. The power source will be a bank of batteries*, or in the future fuel cells. The motor speed will probably be controlled by a solid-state switching device (19) that operates, for example, by turning the power source on and off cyclically at a constant frequency but with variable on-period.

---

* The use of a flywheel for storing energy to propel an electric automobile has been proposed recently (50). An optimally-designed flywheel made of Fiberglas and rotating at 38 000 rpm could store, on a weight basis, 20 times as much energy as the lead-acid battery.

1.4. Current Collectors for a Homopolar Motor

The homopolar motor has a long history dating back to 1831 when Faraday demonstrated the principle of electromagnetic induction by rotating a metal disc in a magnetic field. Despite this, it has not yet found widespread use, largely because of the problem of current collection. The large rotor current, typical of this type of machine*, poses a serious problem for the current collector. If the ohmic loss (I^2R) of the collector is to be tolerable, the collector must have very low resistance. To date, there is no completely satisfactory current collector for the homopolar motor.

Current collection in the homopolar machine can be effected by using brushes and slip-rings (Fig. 3a). Steel and copper, both of which can withstand higher peripheral speeds**, are the materials commonly used for slip-rings (21,22); graphite or metal-impregnated graphite is usually used for brushes. Excessive brush wear is avoided by limiting the operating speed,for the copper-graphite brush, to about 30 m/s when in continuous operation (23). The normal operating speeds for natural graphite or electrographite brushes are higher, 40 to 60 m/s. However, these suffer the drawbacks of relatively low operating current density and high contact voltage (typically 110 kA/m^2 and 2 V) in comparison with the copper-graphite brushes (e.g. 220 kA/m^2 and 0.25 V). Except in an elaborate design (24), graphite or metal-graphite brushes are not suitable for use in a homopolar motor because of its high-current and low-voltage characteristics*.

---

* For example, 6 kA and 1 V (25).

** Copper at a working stress of 7.6×10^7 N/m^2 (5 tons/in^2) can withstand a peripheral speed of about 100 m/s (25).

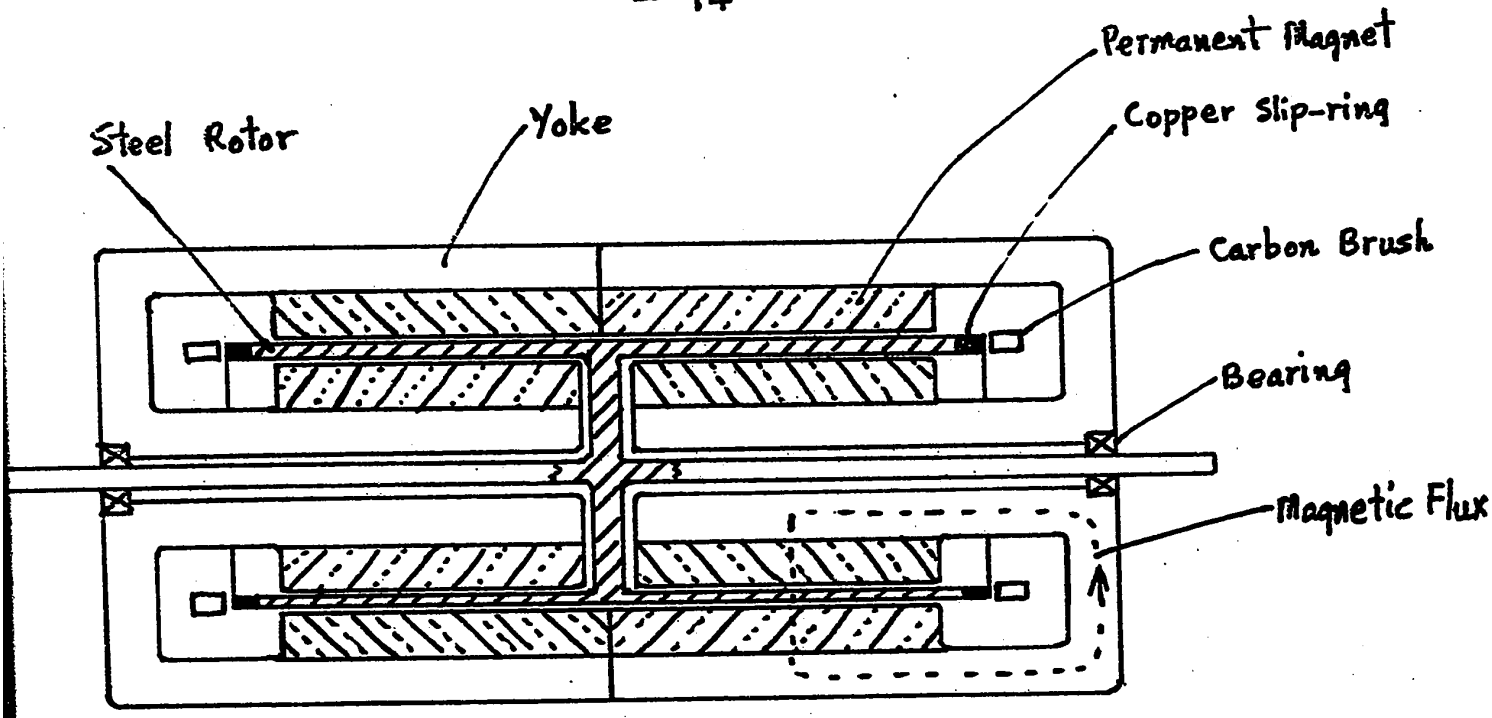

(a)

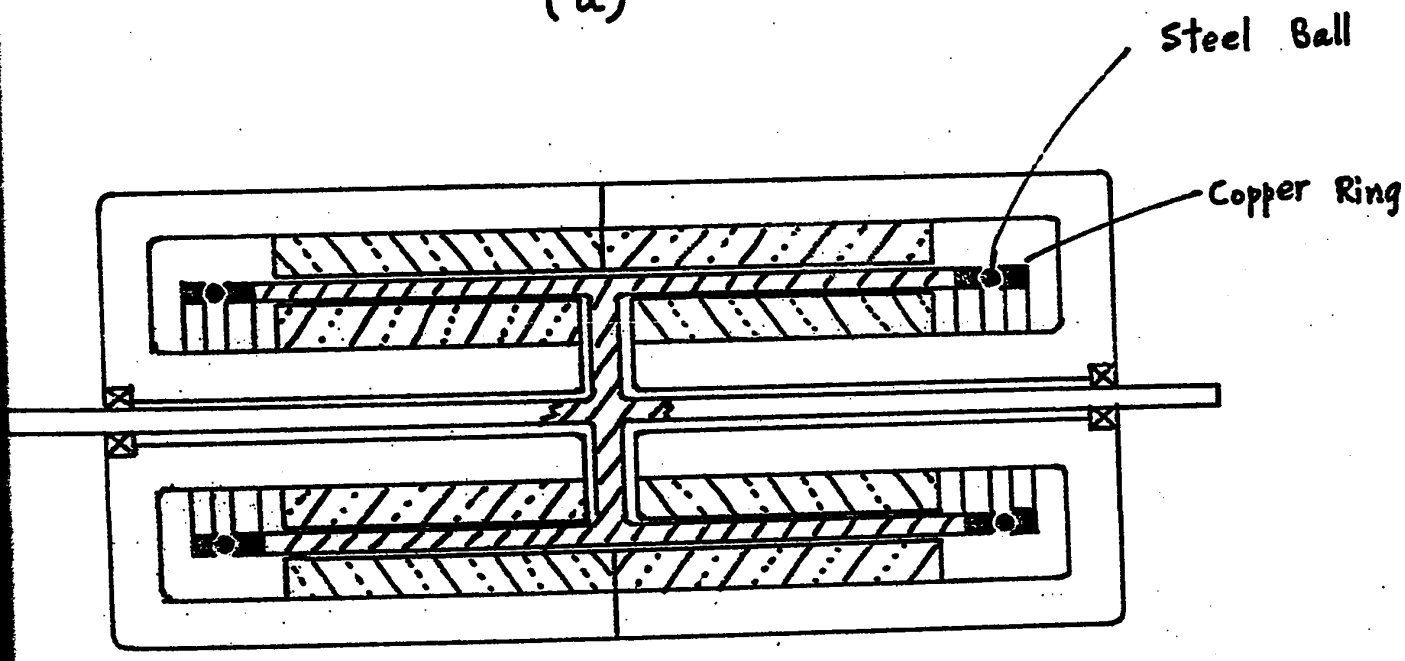

(b)

Fig. 3: A Homopolar Motor — Tentative Design for Automobile Propulsion

(a) with carbon brushes & copper slip-rings

(b) with steel balls & copper rings

Significant advantages can be gained by using liquid metal as the brush material. Not only may the operating current density for the liquid-metal brush be increased to about 5000 kA/m^2 (20,26), but, most important of all, the contact voltage may be reduced to a few millivolts (25). Furthermore, the ohmic loss due to the resistance of the brush material is much smaller because the liquid metal is a better conductor than graphite by a factor of about 300. Due to these excellent characteristics of the liquid-metal brush, the efficiency of the homopolar machine can be as high as 98% (27).

The use of liquid-metal brushes has by no means completely solved the problem of current collection in homopolar machines. Indeed, they introduce problems of their own. Commonly used liquid metalsfor current collection are mercury, NaK (the eutectic of sodium and potassium), and GaIn (the eutectic of gallium and indium). None of these are without drawbacks. Mercury vapour is toxic, and its cummulative effects are fatal. NaK is highly reactive, and has to be handled with extreme caution. Although GaIn is considered safe to handle, our experience has shown that it degrades rapidly from reaction with the atmosphere when in operation. In order to maintain the efficiency of the liquid-metal brush of GaIn, it would be necessary to purify this metal continuously by circulating it through an auxilliary purifier--an uneconomical complication.

In view of the above drawbacks, it seems that the use of liquid-metal brushes would be limited to large power generators in the megawatt range (27,28), or to special devices such as high power density torque converters (26), marine-propulsion systems, and power supplies for electrolytic processes. For such installations, the advantages gained by using such brushes far outweigh the disadvantages. We do not foresee using liquid-metal brushes in homopolar motor for automobile application. Thus,

the need exists to develop an appropriate current collector for use in a homopolar motor for propelling an automobile.

The sliding motion between a rotating slip-ring and a stationary carbon brush (Fig. 3a) causes friction and wear. The brush and slip-ring, however, could be replaced by a set of metal balls placed between two metal races (Fig. 3b). By so doing, the sliding motion is replaced by a rolling one, thus reducing the friction and wear. A possible disadvantage arises, because, as the ball makes contact with both races, two contact interfaces are created, as compared with only one in the case of the brush and slip-ring contact. Since an additional contact interface contributes further contact resistance, its presence is definitely undesirable. Fortunately, experiments with freshly cleaned and stationary silver or gold contacts under light load (0.001-0.002 N) have shown that their contact resistances are less than those of carbon contacts by three orders of magnitude (29). Therefore, the combined resistance of the two metal-to-metal contacts would still be much less than the resistance of a single carbon-to-metal contact.

Ideally all of the balls should be of exactly the same diameter so that they can be in contact with both grooved tracks simultaneously (Fig.3b). In practice, the diameters of the balls vary slightly due to variations in manufacture. The separation between the two races is determined by the diameters of the larger balls, and the smaller ones may not touch both races at the same time. To overcome this problem, we propose to coat the tracks with a low-melting-point alloy, which will be melted by the heat generated by the current*, and will act as a cushion. As the balls roll, the liquid metal will deform, and the work done in deforming it will

---

* See Sect. 4.4.3.

appear as friction. The thicker the layer of liquid metal, the more severe the deformation will be, and the larger the friction. On the other hand, the actual contact area will be larger, and therefore the contact resistance smaller, if the layer is thicker. The best compromise between these two need to be determined.

Due to the lack of a sliding motion which, through wear, generates new surfaces, the self-cleaning action of a rolling contact is expected to be poor. Consequently all of the contact surfaces should be wetted by, or totally immersed in, oil to protect newly-generated surfaces from oxidation. An insulating oil will, at the same time, reduce arcing.

The purpose of this thesis is to study the use of liquid-metal-wetted rolling contacts for current collection, to devise liquid-metal-wetted rolling-contact current collectors, and to assess their practicability.

II. Review of Literature

There is an abundance of literature on electric contacts (30, 47), but it deals almost exclusively with stationary contacts and sliding contacts. There has been very little research on the electrical aspects of rolling contacts, and, to the author's knowledge, no serious study* has been made of applying rolling contacts for transferring large currents. In the following we will review the previous work concerning rolling contacts.

The lubrication of a bearing can normally be described as fluid-film or boundary. Fluid-film lubrication refers to the case when the surfaces in relative motion are completely separated by the lubricant; boundary lubrication to the case when there is some direct contact between the surfaces. The mode of lubrication of a ball bearing in operation has been studied by measuring its electrical resistance (32). This resistance was high when the bearing carried no load, indicating the presence of fluid-film lubrication, but decreased when a load was applied, indicating a change to boundary lubrication. The current carried by the bearing caused corrosion. Mecke observed that the corrosion became considerable when the current was of the order of 10 A (32).

Lidenblad described, in a patent (33), the use of rolling contacts to provide electrical continuity between movable members. His invention probably derived from a design for generating pulses of short duration and high power for radar application. One possible application

---

* According to Holm (31), metal rollers had been used as current collectors in dynamos at the end of the nineteenth century, and Meyer had measured the contact resistance between steel balls.

of his invention, as he suggested, concerned current collection in electric machines, as illustrated in Fig. 4. The use of springy belts in this application appears to be impractical. The output current of the generator passes through the belts and will normally be sufficient to soften them after a short time. The loss of springiness by these belts will result in a disruption of the current.

In oceanographic studies, some of the data to be collected are the temperature and salinity of the sea water at various depths and locations. These can be measured from an ocean vessel by submerging a probe that carries the appropriate sensors. The electrical signals (typically less 100 μV) from them are transmitted by a cable to the on-deck readout system (Fig. 5a). Continuous readout as the cable is wound on a rotating drum is obtained by means of a rotatable contact at the end of the cable. Dauphinee et al. developed a rolling contact device (Fig. 5b), giving thermal emfs of a few tenths of a microvolt and resistance variations less than 0.01 Ω (34,35).

McNab et al. (23) considered using ball or roller bearings, as well as copper leaves, wires or braids, for current collection. However, it is not clear if they experimented with these bearings for transferring current.

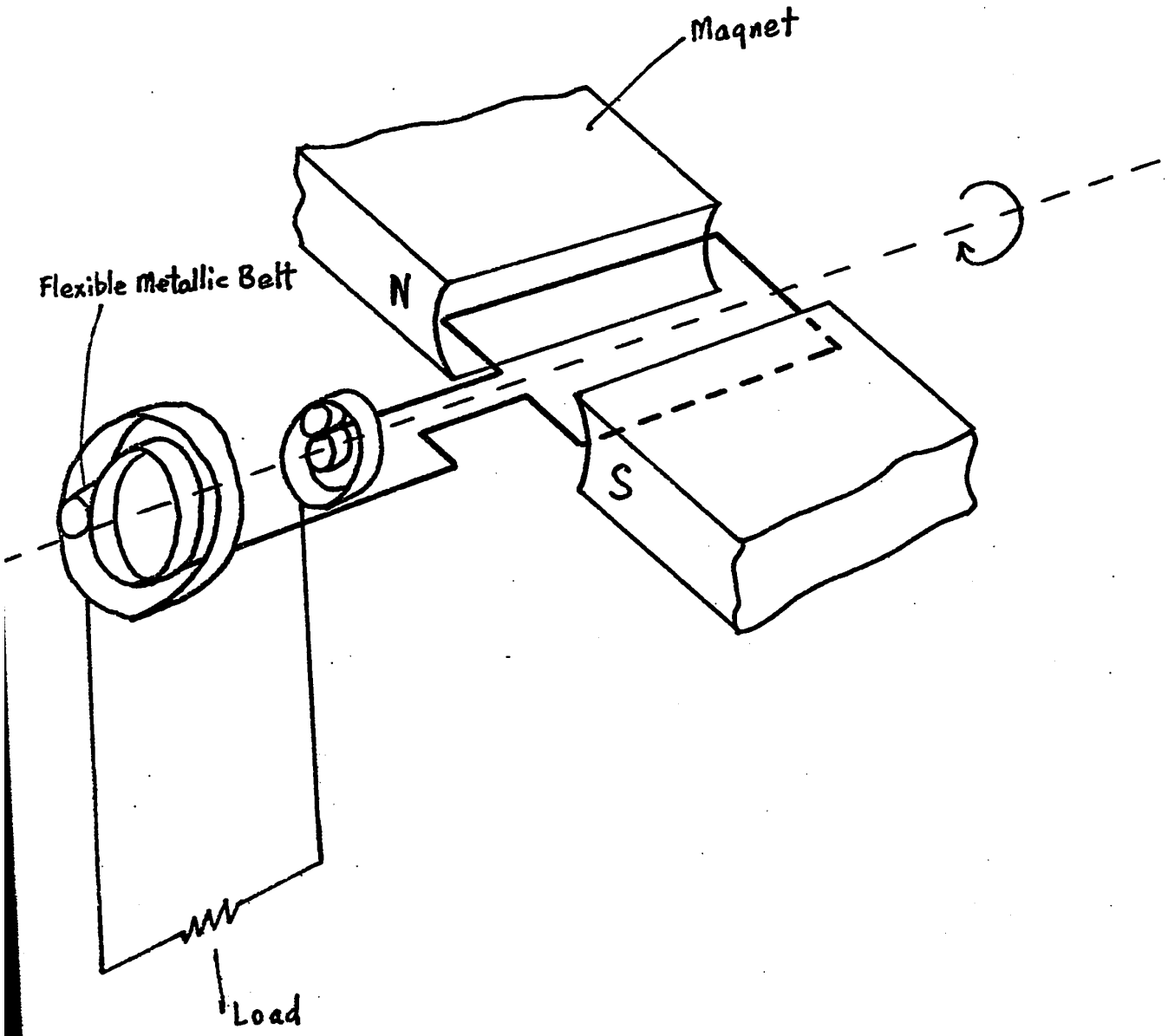

Fig. 4: An Elementary a.c. Generator using Rolling-Contact Current Collectors

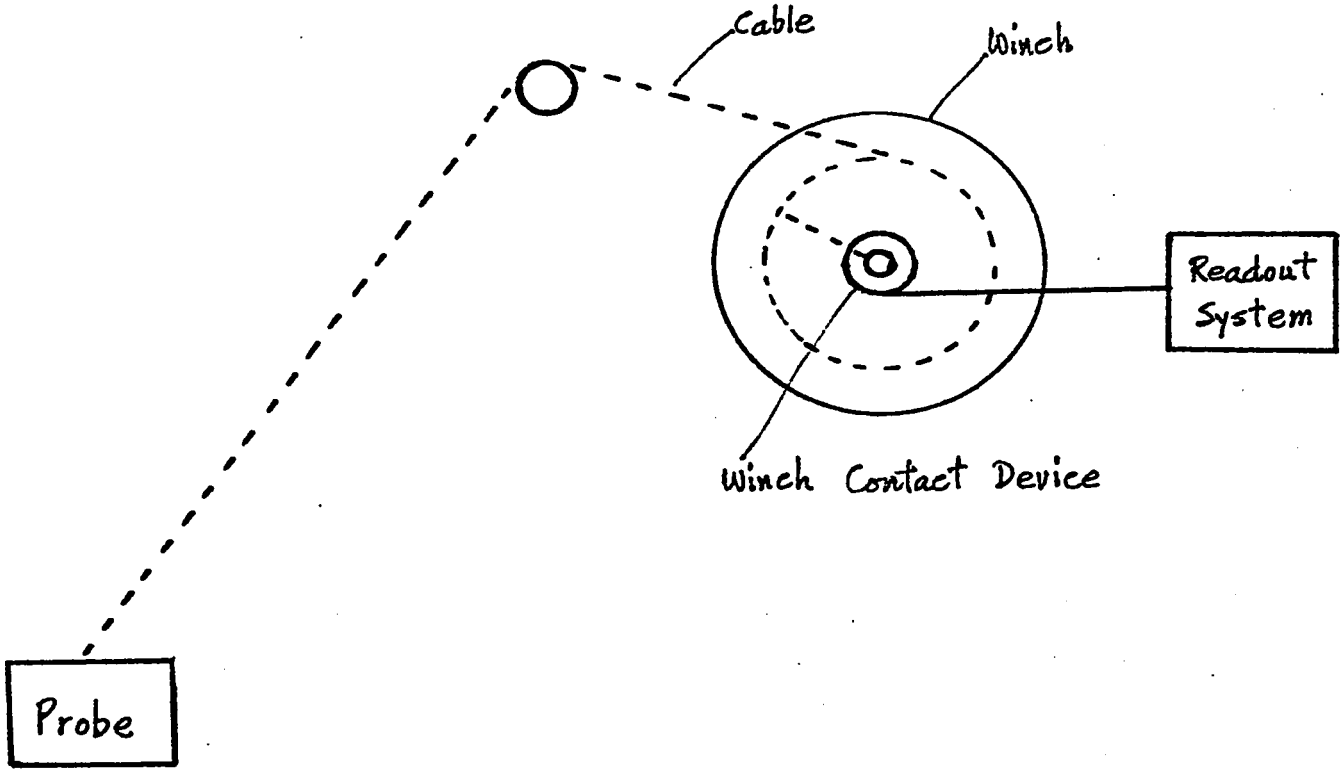

Fig. 5a : Undersea Measuring System

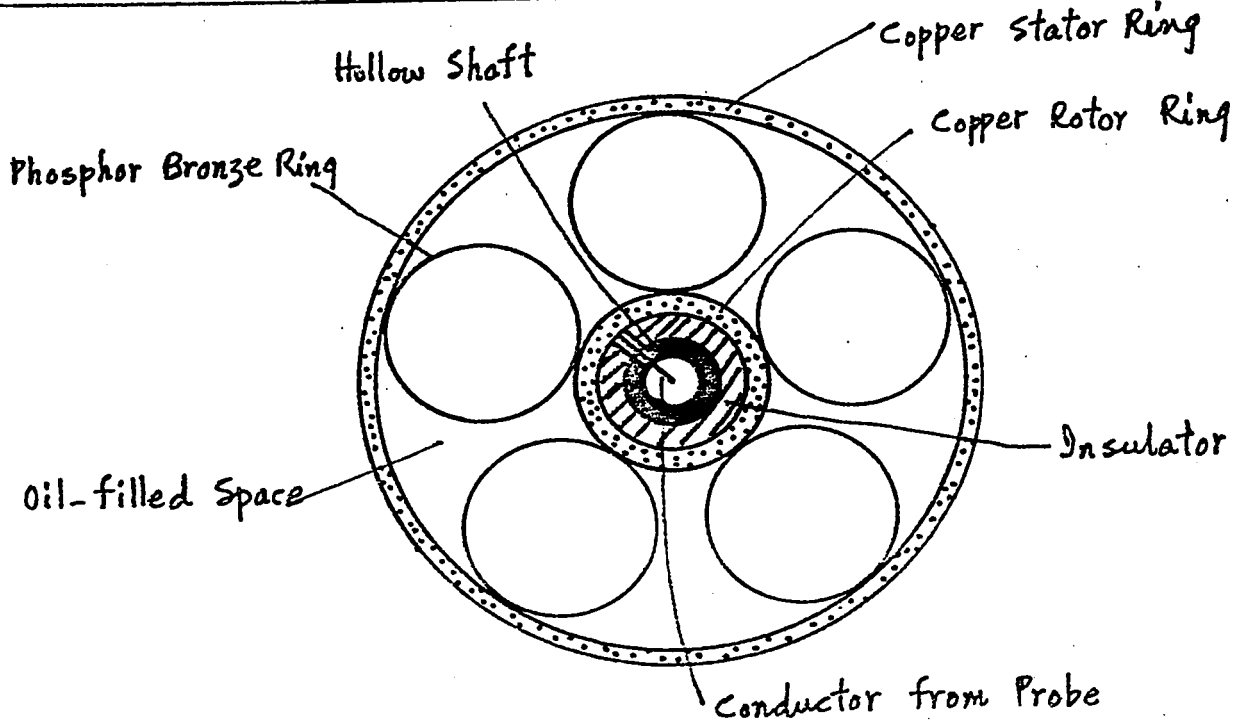

Fig. 5b : Details of Winch Contact Device

III. Theoretical Considerations

3.1. Nomenclature and Nature of Contact

In the nomenclature* used in the literature on electrical contacts the term "contacts" means the junction between two conducting members physically touching each other. Provided no misunderstanding will arise, these members themselves are also called the "contacts". The voltage across the contact interface is called the "contact voltage".

A macroscopically smooth flat surface possesses humps and valleys, or asperities, on a microscopic scale. When two such surfaces are brought into contact, some of the asperities touch each other. The force bringing them together is usually referred to as the contact load, and, in most practical cases, is sufficient to cause the asperities to deform elastically or plastically, thus generating a number of tiny contact areas, or spots. Since the contact load is borne over these areas, they constitute what is called the load-bearing area. The local pressures at the contact spots may not be the same, as there may be elastic deformation at one spot and plastic deformation at another. A contact spot may be partially conducting, when it is partly covered by an insulating film, or wholly conducting, when it is clean. If the film is less than 0.002 μm thick, as in the case of a layer of chemisorbed oxygen atoms, it can usually be penetrated by electrons due to the tunnel effect (36). Thick films such as visible tarnish are practically non-conducting (Fig. 6).

---

* The nomenclature here follows that of Holm (36).

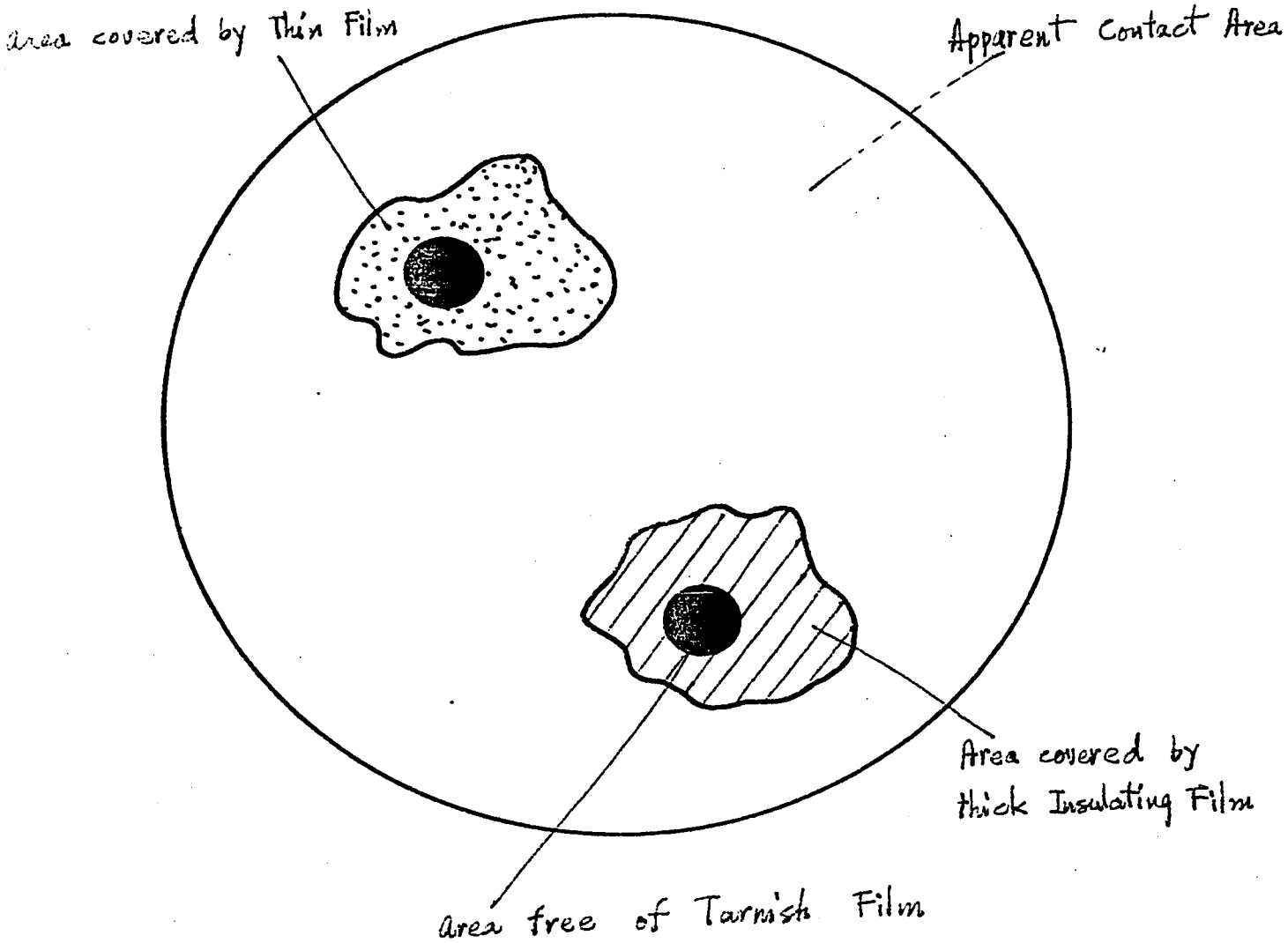

Fig. 6: Nature of Contact

3.2. Contact Area of a Ball pressing against a Plane Surface

One of the important factors determining the resistance of a contact is the actual contact area. Since most of the experiments in this work are concerned with a ball rolling on a surface, we must determine the magnitude of the contact area for such a case.

When two elastic spherical bodies of radii r_1 and r_2 respectively are pressed against each other under a light load P (Fig. 7a), they deform where the contact is made, the intersection being a circle of radius a. If a is much less than r_1 and r_2, it is given by Hertz's formula, as cited by Holm (38),

$$a = \left[\frac{3}{4} P \left(\frac{1 - \upsilon_1^2}{E_1} + \frac{1 - \upsilon_2^2}{E_2} \right) \left(\frac{1}{r_1} + \frac{1}{r_2} \right)^{-1} \right]^{\frac{1}{3}} \qquad (3.1)$$

where υ_1 (υ_2) is the Poisson's ratio and E_1 (E_2) is Young's modulus for the material of sphere 1 (2).

This formula can be applied to the case of a ball pressing against the plane surface of a body (Fig. 7b) by letting one of the radii, say r_1, be infinitely large. Eq. (3.1) then becomes

$$a = \left[\frac{3}{4} P \left(\frac{1 - \upsilon_1^2}{E_1} + \frac{1 - \upsilon_2^2}{E_2} \right) r_2 \right]^{\frac{1}{3}} \qquad (3.2)^*$$

Eq. (3.2) can be rewritten in the form

$$a = k (P r)^{\frac{1}{3}} \qquad (3.3)$$

where $$k = \left[\frac{3}{4} \left(\frac{1 - \upsilon_1^2}{E_1} + \frac{1 - \upsilon_2^2}{E_2} \right) \right]^{\frac{1}{3}} \qquad (3.4)$$

and r = radius of the ball

---

* This also appears in Ref. (39).

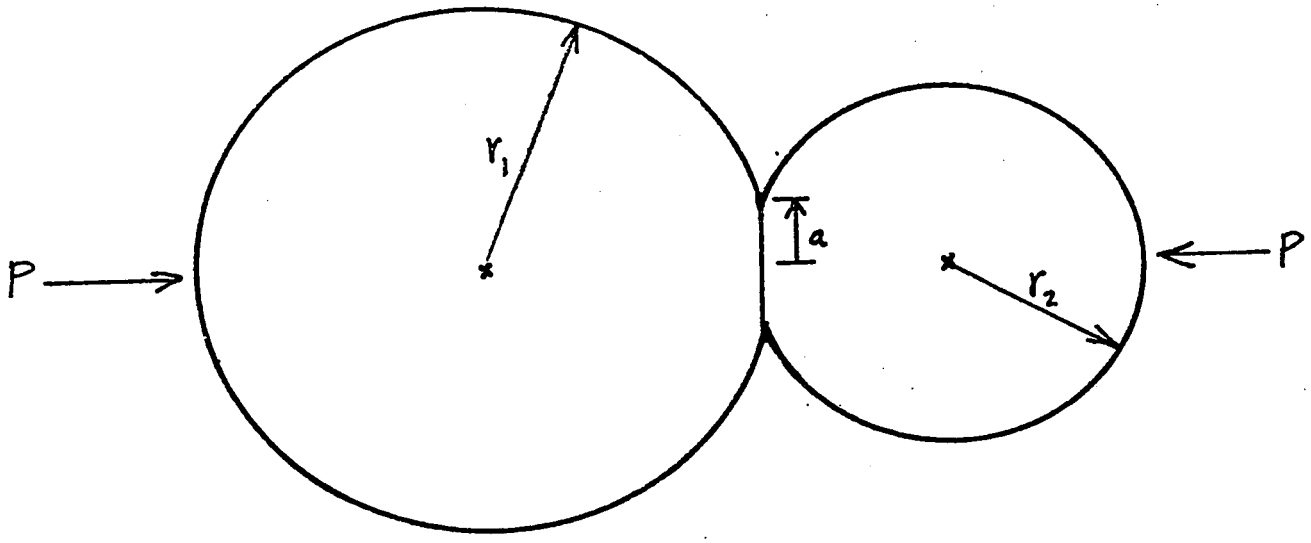

Fig. 7a : Two Elastic Balls in Contact

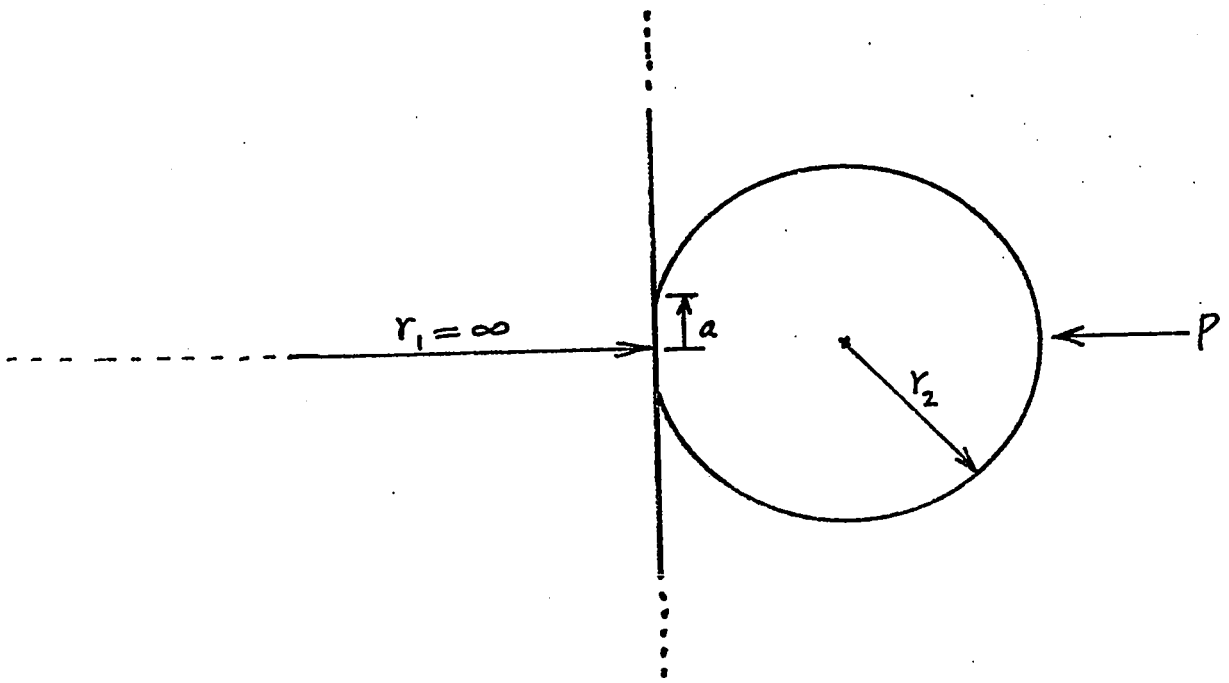

Fig. 7b : An Elastic Ball in Contact with a Plane Surface

3.2.1. Numerical Example

Consider a stainless steel ball resting on a brass surface (Fig. 7b). Taking υ_1=0.33 and E_1=117 × 10^9 N m^{-2} for brass (40), and assuming υ_2=0.29 and E_2=200 × 10^9 N m^{-2} for stainless steel, we obtain from Eqs. (3.4) and (3.3)

$$k = 2.1 \times 10^{-4}$$

$$a = 2.1 \times 10^{-4} \left(P r \right)^{\frac{1}{3}} \quad m$$

If r is 0.0016 m (≈ 1/16 in) and P is 0.1 N (approximately equivalent to a 10-gram weight), then

$$a = 1.1 \times 10^{-5} \quad m$$

This is approximately 1/50 of the radius of a No. 18 AWG copper wire.

3.2.2. A Design Criterion for the Rolling-Contact Current Collector

Consider the two cases as illustrated in Fig. 8. The contact area of each ball-to-disc contact in case (a) is $A_a = \pi k^2 \left(\frac{P}{2} \xi \right)^{\frac{2}{3}}$, and that in case (b) is $A_b = \pi k^2 \left(P 2 \xi \right)^{\frac{2}{3}}$. The total contact areas in the two cases are $4A_a$ and $2A_b$ respectively. The volume needed to accommodate the two balls in case (a) is $V_a = \pi \left(2 \xi \right)^2 2 \xi$ *, and that in case (b) is $V_b = \pi \left(2 \xi \right)^2 4 \xi$. On a per unit volume basis, the ratio between the total contact areas in the two cases is

$$\frac{4 A_a / V_a}{2 A_b / V_b} = 2^{\frac{2}{3}} = 1.59$$

Therefore, case (a) utilizes space better. In a machine where the space for the rolling-contact current collector is limited (Fig. 3b), it is more advantageous to use a larger number of small balls than a smaller number of large balls.

---

* This is being generous.

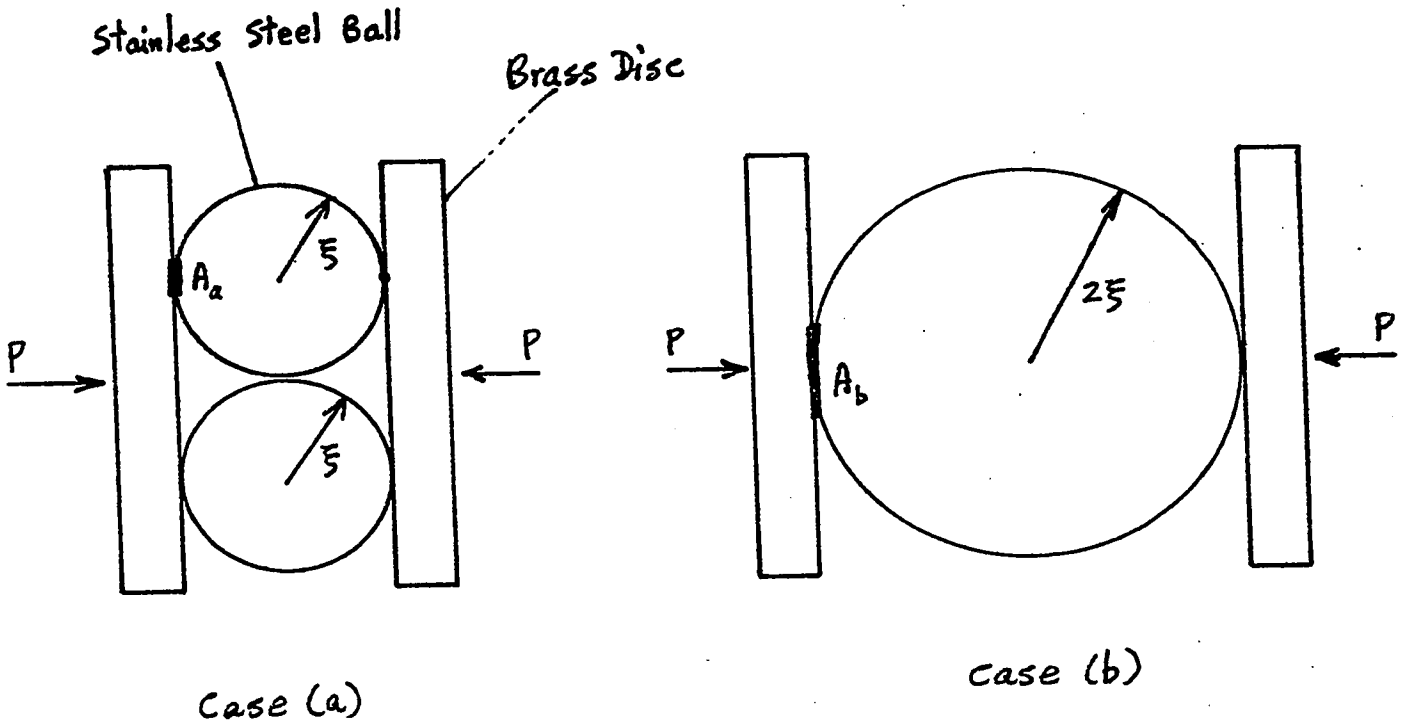

Fig. 8 : Comparison of Total Contact Area for two Cases of Contact

3.3. Electrodynamic Forces on Contacts

When a pair of contact surfaces physically touch each other, "constrictions" are formed at the spots at which they are in contact. One of these is depicted in Fig. 9. The conduction of current between the surfaces is through these constrictions, so-called because the current becomes constricted when going through them. It is known (41,42) that the presence of current constriction gives rise to forces which tend to pinch the constrictions, and to repel the contact surfaces further apart. The combined effect is to break the contact.

3.3.1. Repulsive Force

Let us follow Dwight's example (42) to derive an expression for the repulsive force.

Consider a cylindrical current-carrying conductor having a tapered portion whose radius increases uniformly from r_1 to r_2 (Fig. 10). We neglect the skin effect, and assume uniform current density, i.e. for any value of x the current density does not vary with r. The current density for the cross-section of radius r is $\frac{I}{\pi r^2}$, where I is the total current carried by the conductor. The current passing through the circle of radius y is $I\frac{y^2}{r^2}$. By applying Ampere's law in circuital form, we obtain the magnetic induction at points distant r from the axis as $\frac{\mu I y}{2 \pi r^2}$.

Consider a straight current path MN carrying a particular current from M to N. Obviously, to satisfy this condition and the uniform current density assumption, its cross-sectional area must increase along MN. An elementary portion of this path has a length of $ds = \frac{dx}{\cos \alpha}$. For every ampere of current it carries, the force on it is

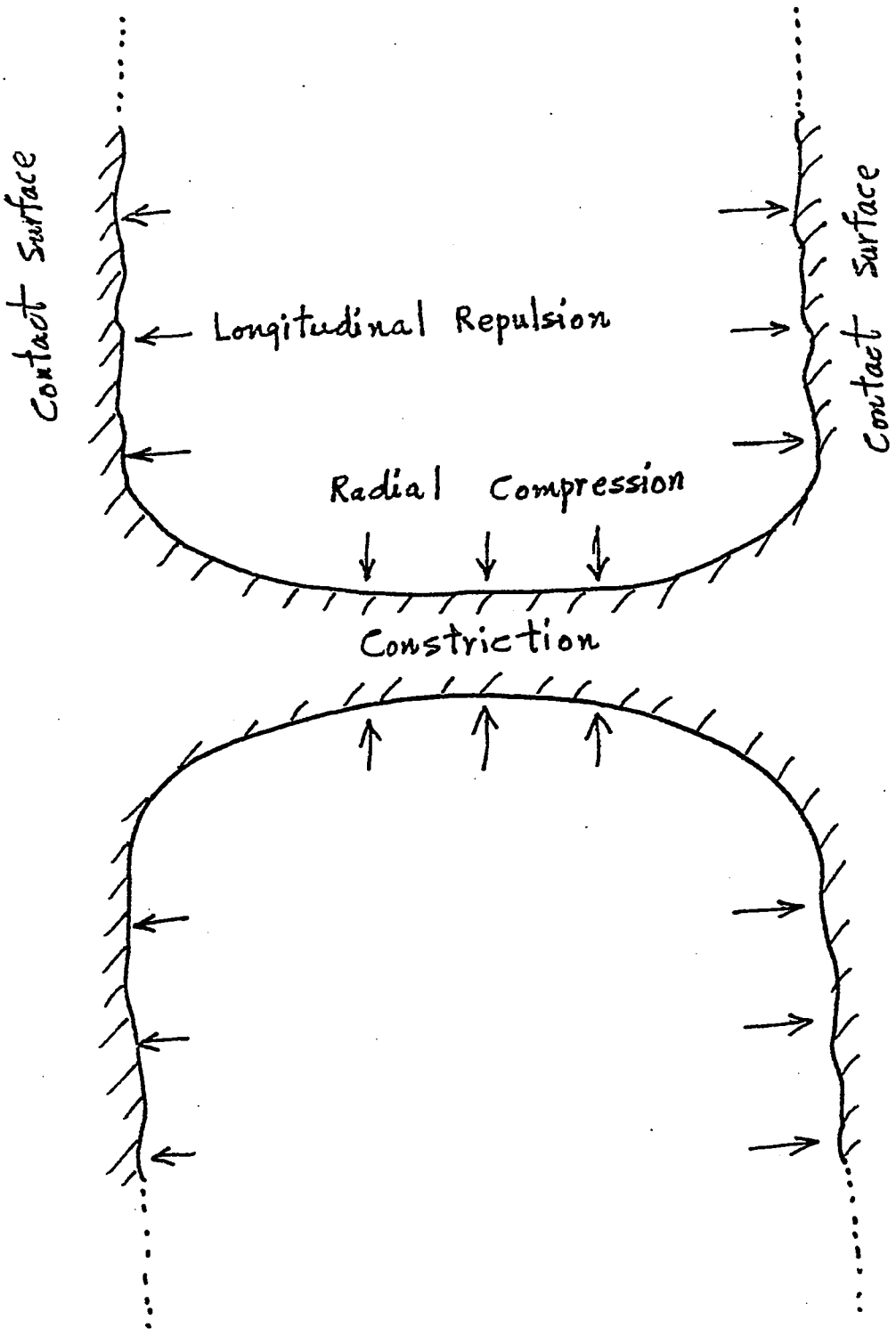

Fig. 9 : Electrodynamic Forces on a Constriction and the Contact Surfaces

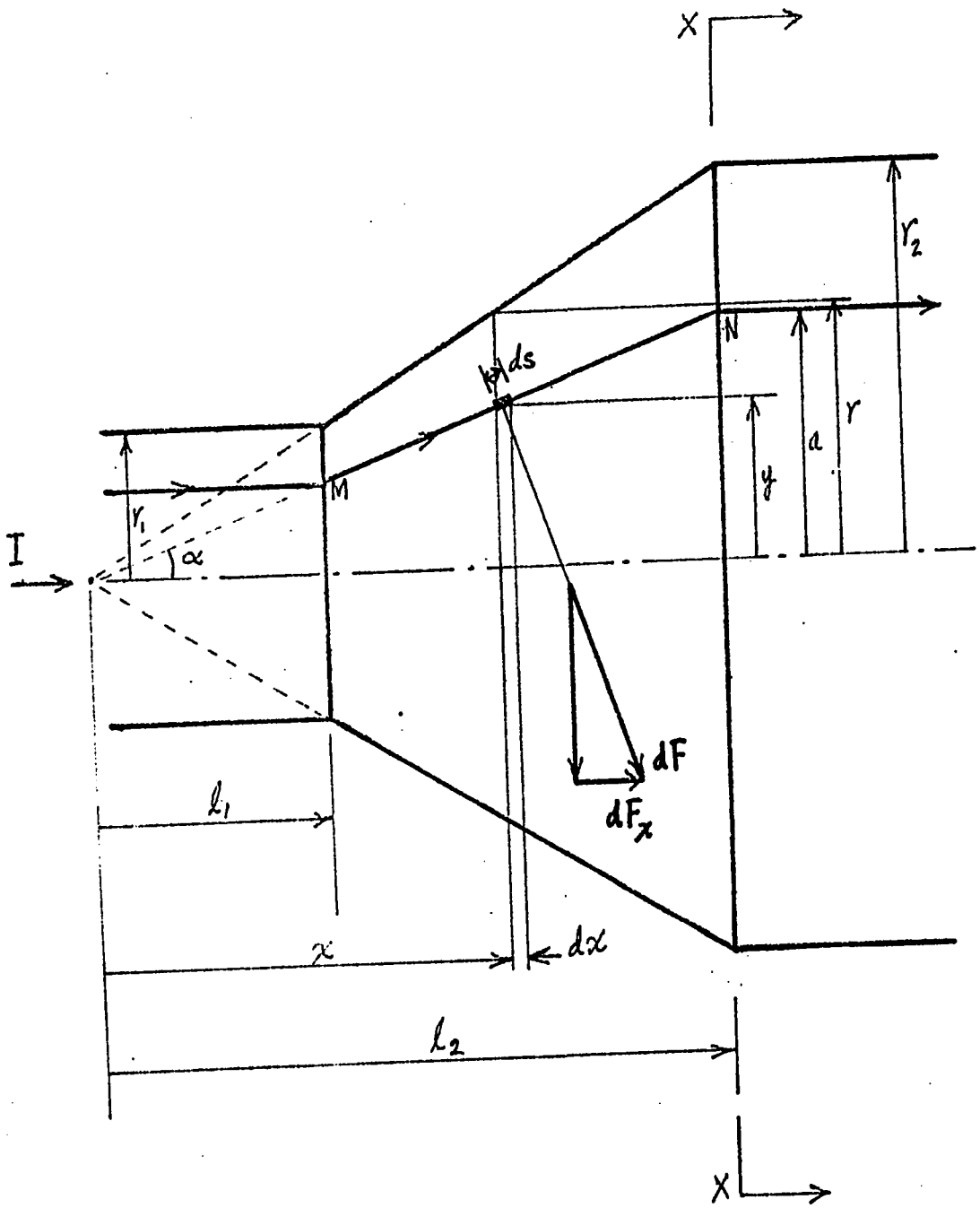

Section through XX

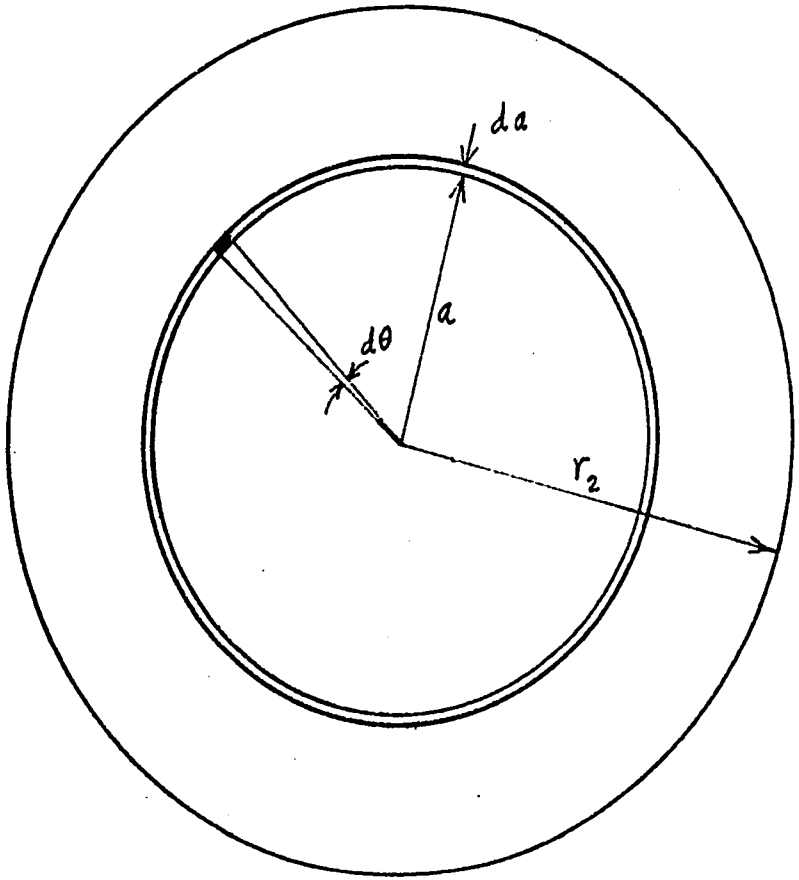

Fig. 10 : A Cylindrical Conductor with a Tapered Portion

$$df = \frac{dx}{\cos \alpha} \frac{\mu I y}{2 \pi r^2} \tag{3.5}$$

The longitudinal component of df is

$$df_x = \sin \alpha \, df = \tan \alpha \, dx \, \frac{\mu I y}{2 \pi r^2} = \frac{dx}{x} \frac{\mu I y^2}{2 \pi r^2} = \frac{dx}{x} \frac{\mu I a^2}{2 \pi r_2^2}$$

The longitudinal component of the total force on the current path MN per ampere of current is

$$f_x = \int_{z_1}^{z_2} df_x = \ln \frac{z_2}{z_1} \frac{\mu I a^2}{2 \pi r_2^2}$$

If similar paths like this make up a thin shell having a cross-sectional area of $2 \pi a \, da$, then the total current carried by this shell is $I \frac{2 a \, da}{r_2^2}$.

The longitudinal component of the total force on this current shell is

$$dF_x = f_x I \frac{2 a \, da}{r_2^2} = \ln \frac{r_2}{r_1} \frac{\mu I^2 a^3 \, da}{\pi r_2^4}$$

The longitudinal component of the total force on the tapered portion of the conductor is

$$F_x = \int_0^{r_2} dF_x = \frac{\mu I^2}{4 \pi} \ln \frac{r_2}{r_1} \tag{3.6}$$

This is the expression given by Dwight. The following are a few important remarks related to it:

(a) μ is the permeability of the material of the tapered portion.

(b) the direction of df remains the same, even if the current flow is reversed. Therefore, the direction of F_x is independent of the direction of the current.

(c) Instead of tapering uniformly, the conductor may change its radius uniformly from r_1 to r_i and then from r_i to r_2. The total longitudinal force on the two tapered portions is

$$\frac{\mu I^2}{4\pi}\left(\ln\frac{r_i}{r_1}+\ln\frac{r_2}{r_i}\right)=\frac{\mu I^2}{4\pi}\ln\frac{r_2}{r_1}$$

Thus, it does not depend on the intermediate radius.

(d) It is important to realize that F_x is obtained by considering the interaction of the current with its own magnetic field. Bron treated the problem differently by considering the magnetic pressure that accompanies a magnetic field, and obtained a slightly different result (Appendix A).

3.3.1.1. Numerical Example

Fig. 11 shows a stainless steel ball in contact with two brass discs parallel to each other. In order to make use of the numerical example in Sect. 3.2.1, we let the radii of the ball and the discs be each equal to r=0.0015975 m, and the contact load be P_0=0.1 N*. Then, the radius of each circular contact area is a_0=1.137079 × 10^{-5} m. If now a current, I, of 10 A ** flows from one disc to the other through the ball, there will be forces acting on them at each disc-to-ball contact due to the current constrictions. However, the forces on the ball are symmetrical about the plane XX, passing through the centre of the ball and parallel to the discs. Therefore, the net force on the ball is zero. The force, F_0, on each brass disc is obtained by applying Eq.(3.6). Since brass and stainless steel are non-magnetic materials, it will suffice to let their permeabilities be each equal to 4 π × 10^{-7} J s^2 C^{-2} m^{-1}. Thus,

$$F_0 = 4.9 \times 10^{-7} \quad \text{N}$$

Since F_0 opposes P_0, the net contact load becomes

$$P_1 = P_0 - F_0 = 0.099\ 999\ 51 \quad \text{N}$$

From Eq. (3.3), the radius of the contact area becomes

$$a_1 = 1.137\ 077 \times 10^{-5} \quad \text{m}$$

Values at successive iterations are shown in Table II. At the 83rd iteration, F_{83} is larger than P_{83}. At this point the contact will open, and there will be no current flow. However, the forces due to current constrictions will also vanish, and the contact will close again, resulting in the bouncing of the contact surfaces.

---

* The implication of the subscript '0' will be apparent later.

** This current is sufficiently large. If the diameter of each of the copper rings in Fig. 3b is 0.1 m, approximately one hundred of the balls considered here can be accommodated by the grooved track of the ring. In this case, the rotor current will be 1000 A if each ball carries 10 A.

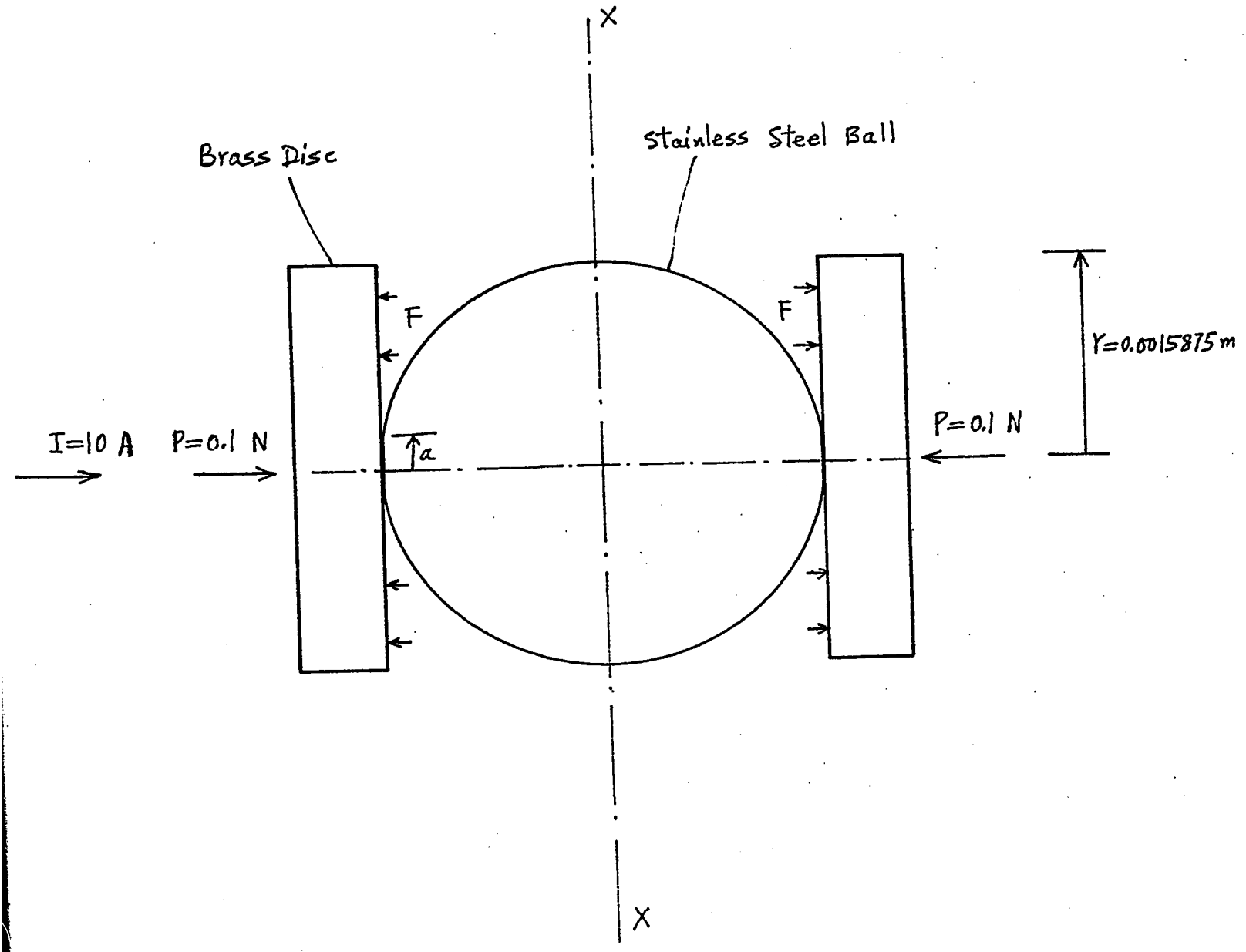

Fig. 11 : A Ball in Contact with Two Discs

Table II

Net Contact Load, Radius of Circular Contact Area, and Repulsive Force on a Contact Surface at Successive Iterations

i	Net Contact Load P_i (N)	Radius of Circular Contact Area R_i (m)	Repulsive Force on Contact Surface F_i (N)
0	0.1000000	0.00001137079	0.0000005
1	0.0999995	0.00001137077	0.0000020
2	0.0999975	0.00001137069	0.0000044
3	0.0999931	0.00001137053	0.0000079
4	0.0999852	0.00001137023	0.0000123
5	0.0999728	0.00001136976	0.0000178
6	0.0999551	0.00001136908	0.0000242
7	0.0999309	0.00001136817	0.0000316
8	0.0998992	0.00001136697	0.0000400
9	0.0998592	0.00001136545	0.0000494
10	0.0998098	0.00001136358	0.0000598
11	0.0997501	0.00001136131	0.0000711
12	0.0996789	0.00001135861	0.0000835
13	0.0995955	0.00001135543	0.0000968
14	0.0994986	0.00001135175	0.0001112
15	0.0993875	0.00001134752	0.0001265
16	0.0992610	0.00001134271	0.0001428
17	0.0991182	0.00001133727	0.0001601
18	0.0989581	0.00001133116	0.0001784
19	0.0987796	0.00001132434	0.0001977
20	0.0985819	0.00001131678	0.0002180
--	----------	----------	----------
--	----------	----------	----------
80	0.0137070	0.00000586279	0.0036750
81	0.0100320	0.00000528347	0.0038363
82	0.0061957	0.00000449930	0.0040411
83	0.0021546	0.00000316408	0.0043875

3.3.2. Constricting Force

Consider a cylindrical conductor of radius R carrying a current I (Fig. 12). As before, we assume uniform current density, $\frac{I}{\pi R^2}$. The current carried by the cylinder of radius r is $\frac{I r^2}{R^2}$. By applying Ampere's law in circuital form, we find the magnetic induction at a point distant r from the axis to be $\frac{\mu I r}{2 \pi R^2}$. The cylindrical shell of length ℓ, and radii r and $(r + \Delta r)$ can be considered to be composed of a large number of current paths each of cross-sectional area ΔA approximately equal to $r \Delta r \Delta\theta$. The current carried by each path is then $\frac{I r \Delta r \Delta\theta}{\pi R^2}$. The force on each path is

$$\Delta F = \frac{\mu I^2 \ell r^2}{2 \pi^2 R^4} \Delta r \Delta\theta \tag{3.7}$$

acting radially inward. It follows that the vector sum of all the forces on the current paths is zero. The force ΔF is distributed over the whole current path and can be considered as due to the pressure difference existing between the outer and inner surfaces of the current shell. It follows that

$$\begin{aligned} \Delta F = F_{r+\Delta r} - F_r &= p_{r+\Delta r} \ell (r + \Delta r) \Delta\theta - p_r \ell r \Delta\theta \\ &\cong (p_{r+\Delta\theta} - p_r) \ell r \Delta\theta = \Delta p \ell r \Delta\theta \end{aligned} \tag{3.8}$$

where p is the pressure.

Comparing Eqs. (3.7) and (3.8), we obtain

$$\Delta p = \frac{\mu I^2 r}{2 \pi^2 R^4} \Delta r \tag{3.9}$$

As Δr approaches an infinitesimal, Eq. (3.9) becomes

$$dp = \frac{\mu I^2 r}{2 \pi^2 R^4} dr$$

The difference in pressure between the axis and the surface of the conductor is

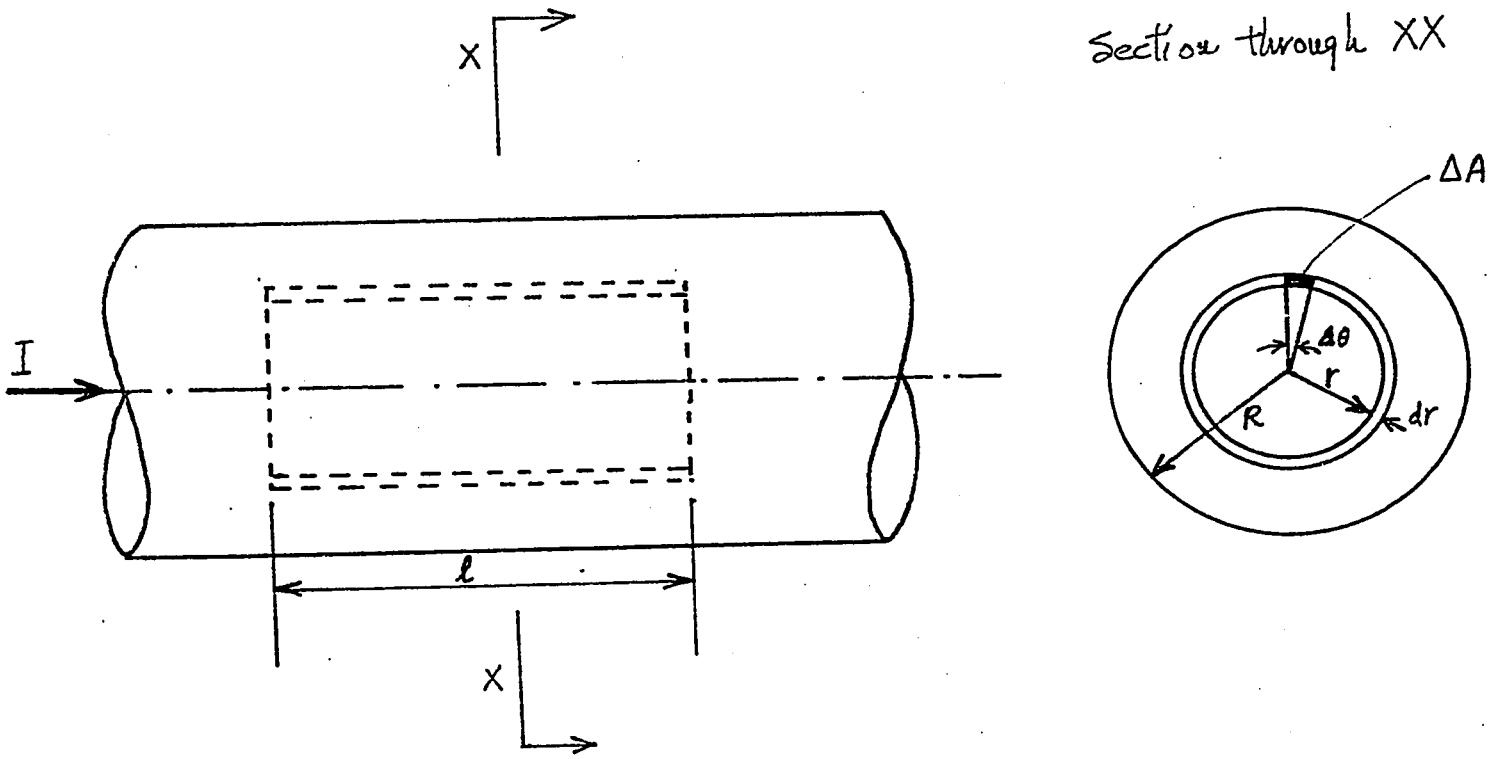

Fig. 12 : A Cylindrical Conductor of Uniform Cross-section

$$P_R = \int_0^R dp = \frac{\mu I^2}{4 \pi^2 R^2} \qquad (3.10)$$

Thus, a current passing through a conductor generates a radial pressure tending to constrict the conductor. This phenomenon is commonly known as the "Pinch Effect". If the conductor is a liquid metal, the pinching will reduce its radius, and in turn magnify the radial pressure until it finally collapses.

3.3.2.1. Numerical Example

Making use of the example in Sect. 3.3.1.1, we let

$\mu = 4 \pi \times 10^{-7}$

$I = 10$ A

$R = 3.16 \times 10^{-6}$ m*

Substituting these values in Eq. (3.10), we obtain the pressure at the periphery of the constriction,

$P_R = 3.2 \times 10^5$ N m^{-2}

This is much less than the ultimate tensile strength of brass ($\sim 40 \times 10^7$ N m^{-2} (43)). Therefore, it will not cause the metal constriction to collapse.

---

* This comes from the last row of Table II.

3.4. Relation between Voltage and Temperature of a Symmetric Contact

When a potential difference is applied across a pair of contacting members, current flows from one member to the other through the constrictions. The temperature of these members rises because of Joule heating and can become so intense that local melting occurs in the constrictions where the current densities are very high. The relation between the voltage across the contact and the constriction temperature has been studied (44,45). A simple one-dimensional analysis of a symmetric contact (Fig. 13) is considered here under the following assumptions:

(a) An equipotential surface is also an isothermal surface. An argument supporting this assumption can be found in Ref. (44).

(b) The medium surrounding the contact members is a perfect electric and thermal insulator, that is, there is no heat or electric leakage to the medium.

(c) Both contact members are isotropic, having the same electrical conductivity σ and thermal conductivity λ.

(d) The contact is symmetric about the plane of contact (x=0).

(e) The temperature in the contact is a maximum at this plane. This also implies that there is no flow of heat across the contact plane.

(f) Thermo-electric effects are ignored.

The rate of heat generated in the region bounded by the contact plane and the surface A is

$$q_e = V\ I$$

where V and I are voltage and current respectively. Since $I = -\frac{dV}{dR}$, and $dR = \frac{1}{\sigma}\frac{dx}{A}$, where R is resistance, then

$$q_e = -\frac{\sigma A V}{dx}\, dV \qquad (3.11)$$

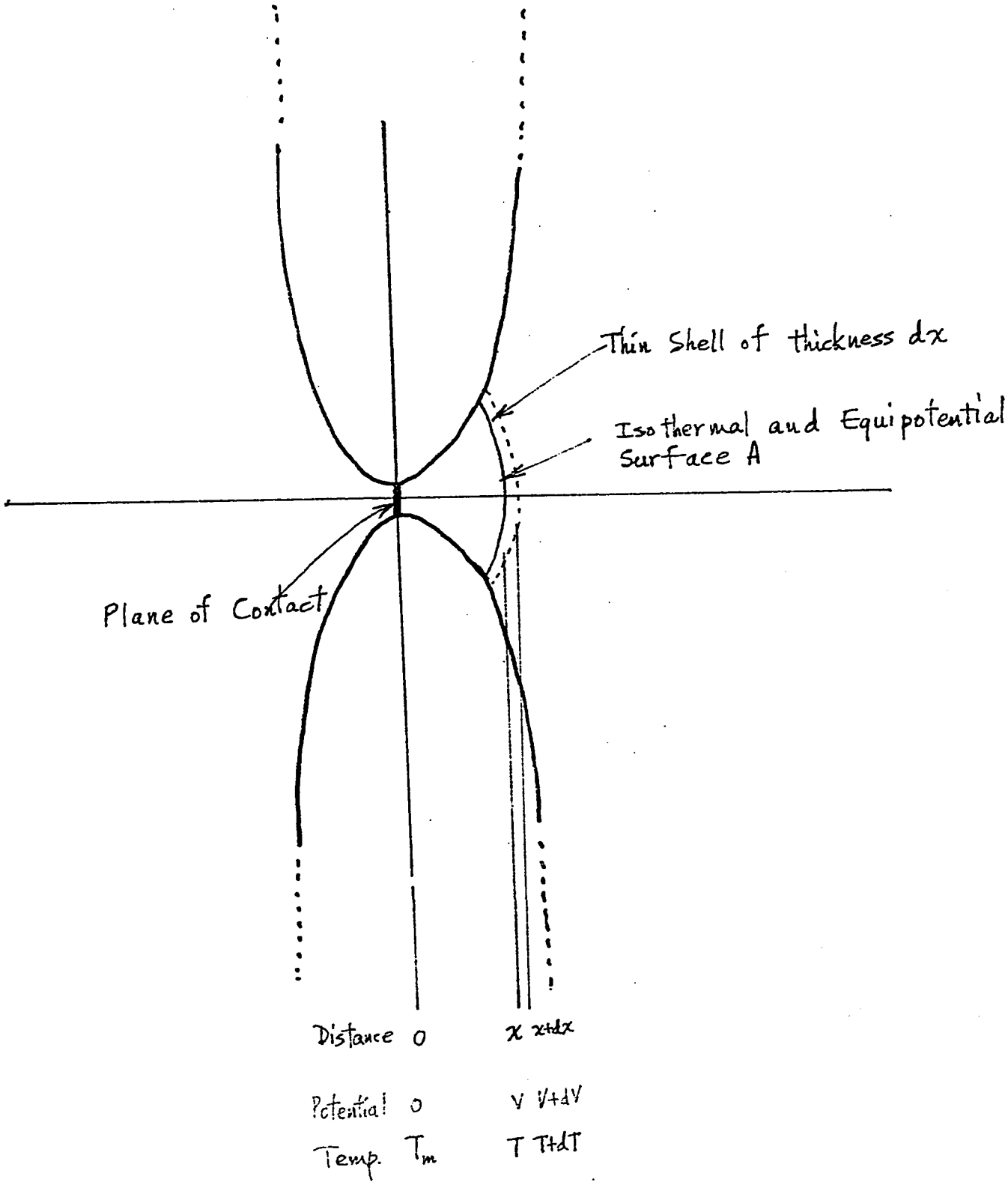

Fig. 13 : A Symmetric Contact

The heat flow across the surface A due to the thermal gradient is

$$q_t = \lambda A \frac{dT}{dx} \tag{3.12}$$

By the aforementioned assumptions, no heat flows across the contact plane nor is lost to the surrounding medium. Therefore, at equilibrium, q_t must equal q_e, and, from Eqs. (3.12) and (3.11),

$$-\frac{\lambda}{\sigma} dT = V\, dV \tag{3.13}$$

Integrating both sides of Eq. (3.13), we obtain

$$\int_T^{T_m} \frac{\lambda}{\sigma} dT = \frac{V^2}{2} \tag{3.14}$$

where T_m is the temperature at the contact plane.

According to the Weidemann-Franz law,

$$\frac{\lambda}{\sigma} = L\, T$$

where L is considered to be constant. After integration, Eq. (3.14) becomes

$$L\,(T_m^2 - T^2) = V^2 \tag{3.15}$$

For metals, a good value for L is $2.4 \times 10^{-8}\ V^2\ K^{-2}$ (44). If the surface A is sufficiently distant from the contact plane, T is equal to the temperature of the bulk material of the contact , T_c, and V is equal to $\frac{V_c}{2}$, where V_c is the voltage across the two contacting members. Substituting for L and V in Eq. (3.15), we obtain

$$T_m^2 - T_c^2 = 1.04 \times 10^7\ V_c^2 \tag{3.16}$$

Assuming T_c to be 300 K, i.e. near room temperature, Eq. (3.16) becomes

$$T_m^2 = 1.04 \times 10^7\ V_c^2 - 9 \times 10^4 \tag{3.17}$$

The value of V_c that causes melting to occur is known as the "melting voltage". In the experiments to follow, we dealt with steel balls,

bare brass surfaces, and brass surfaces coated with Wood's Metal. The melting voltages for these materials, calculated according to Eq. (3.17), are tabulated in Table III.

Table III

Melting Voltages of Steel, Brass, and Wood's Metal

(Temperature of Bulk: 300 K)

Material	Composition (%)	Melting Point (^{o}C) (40)	Melting Voltage (v)
Steel	99 Fe, 1 C	1430	0.519
Brass	67 Cu, 33 Zn	940	0.364
Wood's Metal	50 Bi, 25 Pb, 12.5 Zn, 12.5 Cd	70	0.052

IV. Experiments and Experimental Results

4.1. Introduction

A number of experiments were performed to provide data for quantitative considerations of the rolling-contact collectors, particularly of those wetted by liquid metal. The experiments were divided into three groups. The first group dealt with the voltage drop across a stationary contact between two discs. The contacting surfaces were bare brass, and also brass coated with Wood's Metal*, an alloy that melts at 70°C. The second group of experiments dealt with the voltage drop across two discs with a steel ball between them. As before, the contact surfaces of the discs were bare brass, and brass coated with Wood's Metal. Both the stationary case, in which the discs and the ball were stationary, and the rolling case, in which one disc rotated and the ball rolled, were studied. The last group of experiments dealt with the voltage drop for three different rolling-contact current collectors: a commercially available ball bearing used as a current collector, and two experimental current collectors, one wetted by the liquid metal, GaIn, and the other by liquid Wood's Metal.

---

* See Table III for its composition.

4.2. Stationary Brass Disc to Brass Disc Contacts at Fixed Contact Load

4.2.1. Bare Surfaces at Fixed Current and Room Temperature

The surfaces of two brass discs of the same dimensions were machined flat in a lathe, and then polished with abrasive paper. The final and finest paper used was a Crocus cloth. During the polishing, the paper was wetted by oil, and was lying on the flat surface of a machine table. The final diameter, thickness, and weight of each disc were 4.7 cm, 1.3 cm, and 0.191 kg respectively. A current lead and a potential lead were soldered to each disc. A brass-to-brass contact was formed by placing one disc coaxially on top of the other (Fig. 14). Thus, the contact load due to the weight of the upper disc was 1.87 N.

First, a current of 1.0 A was passed through the contact from a regulated dc power supply (Kepco CK18-3M), and the voltage across the discs was measured. Then the upper disc was raised, rotated by approximately 30 degrees, and replaced. With the current still at 1.0 A, the voltage was again measured. The above procedures were repeated until a total of 79 readings were obtained. These measured voltages ranged from 0.4 V to 3.5 V. This range was divided into 31 equal intervals. The number of voltage readings (normalized with respect to their maximum) in each 0.1 V interval is plotted in Fig. 15(a) as a function of the voltage. The distribution shown has a peak between 1.0 and 1.1 V.

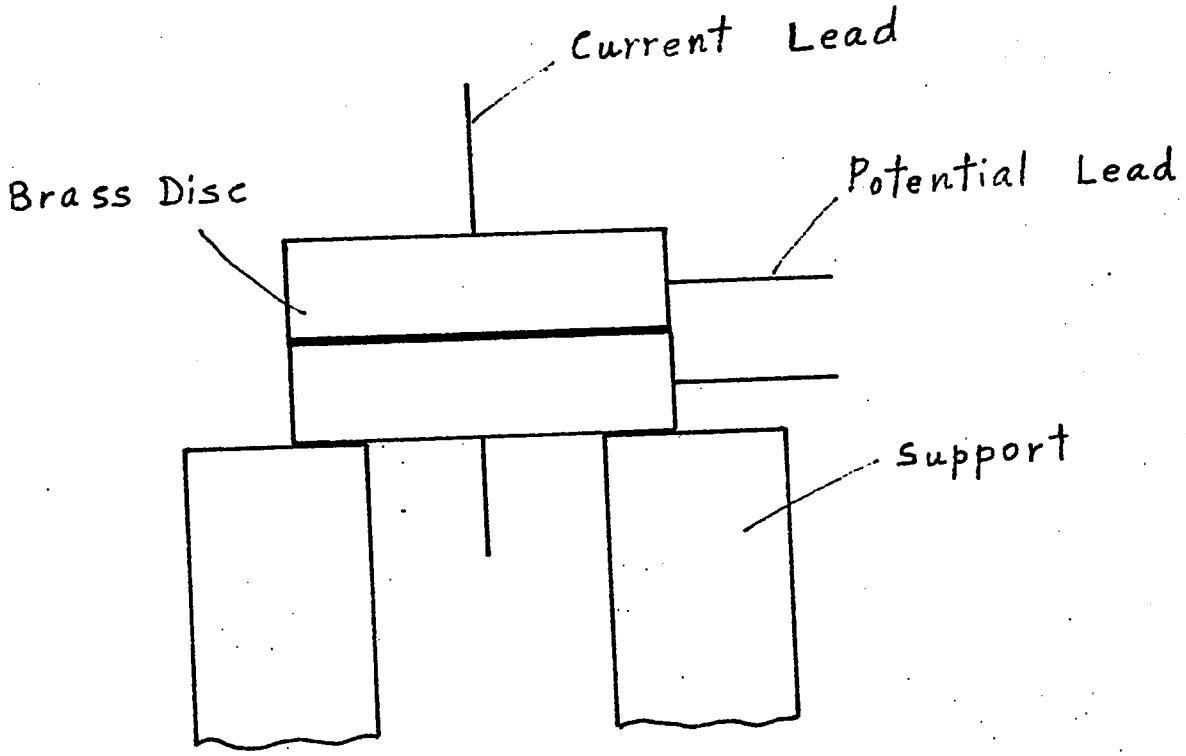

Fig. 14: Experimental Setup for studying Stationary Contacts

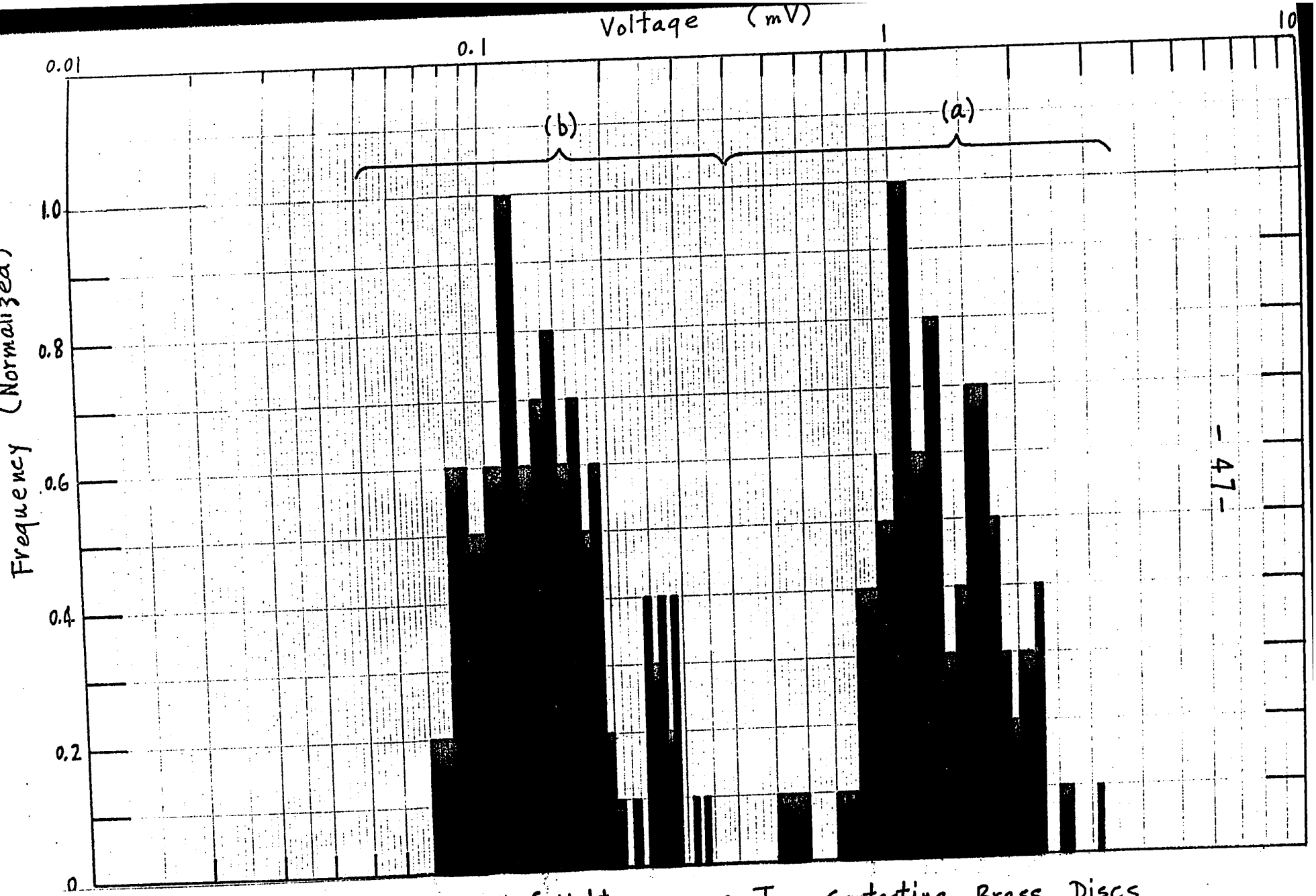

Fig. 15: Distribution of Readings of Voltage across Two Contacting Brass Discs

(a) Bare Surfaces, (b) Surfaces coated with Wood's Metal about 0.01 mm thick

(Dia of each disc = 4.7 cm ; Current = 1.0A ; Contact Load = 1.87 N)

4.2.2. Bare Surfaces at Varying Current and Room Temperature

Using the same experimental setup as in Sect. 4.2.1, the current was increased from 0 to 1.0 A and back again in steps of 0.2 A. The voltage across the brass discs was measured at each step, giving a set of voltage and current readings. As before, the upper disc was raised, rotated, and replaced on the lower one. Again, a set of voltage and current readings was obtained. These procedures were repeated to give a total of three sets of readings, shown in Fig. 16(a).

For each individual set, the points fall closely on a straight line, showing that each individual contact was ohmic, i.e. voltage is proportional to current, and that the measurements were reproducible.

4.2.3. Surfaces coated with Wood's Metal at Room Temperature

The contact surfaces of the two brass discs used in Sect. 4.2.2 were each coated with a layer of Wood's Metal about 0.01 mm thick. The measurements described in Sects. 4.2.1 and 4.2.2 were repeated with the results shown in Figs. 15(b) and 16(b).

It is evident that the presence of Wood's Metal reduced the voltage across the brass discs.

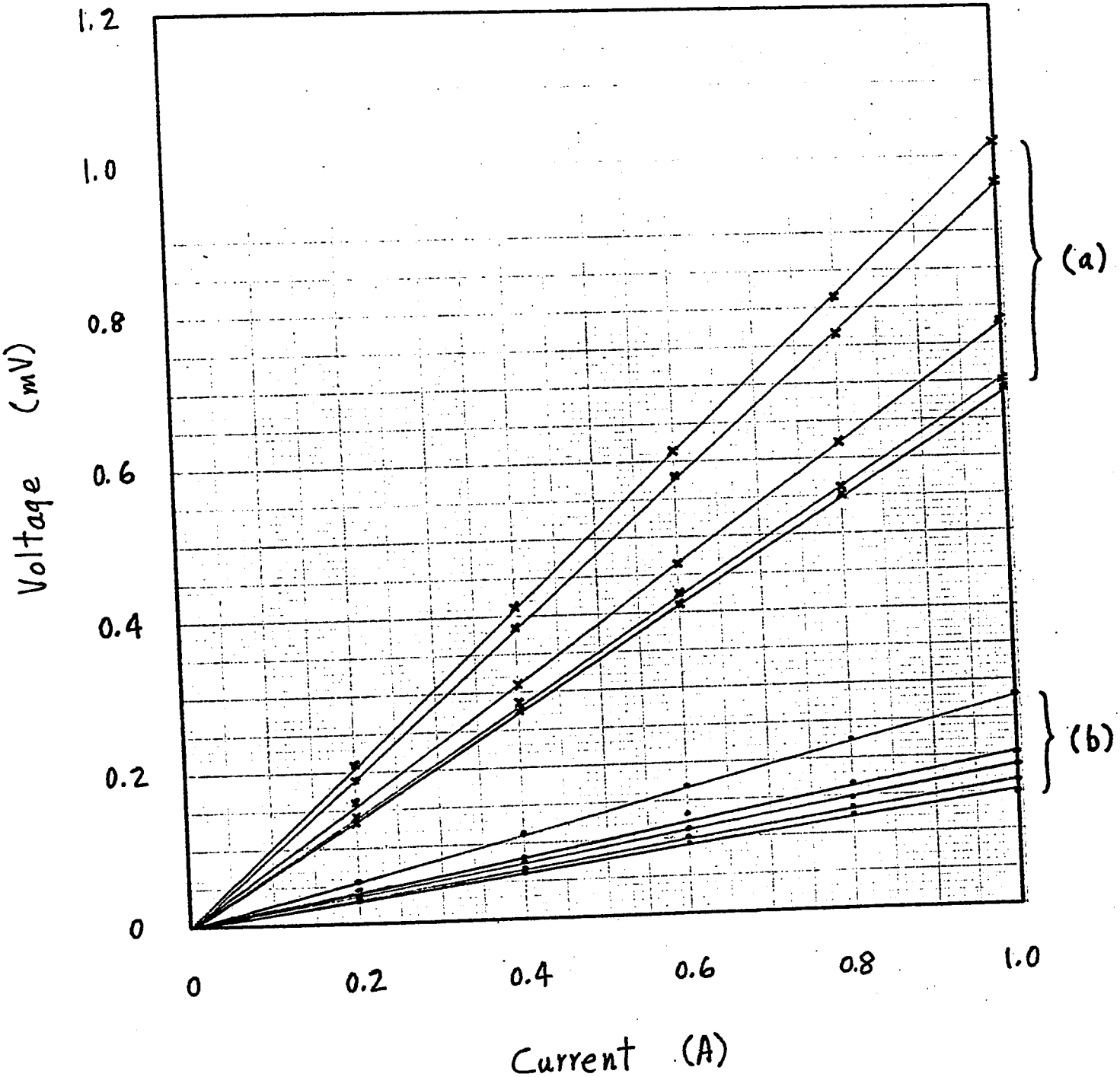

Fig. 16: Voltage across Two Contacting Brass Discs at Varying Current

(a) Bare Surfaces, (b) surfaces coated with Wood's Metal about 0.01 mm thick

(Dia of each disc = 4.7 cm; Contact Load = 1.87 N)

4.2.4. Surfaces coated with Wood's Metal at Fixed Current and Elevated Temperatures

4.2.4.1. Thin Coating

The experimental setup used in Sect. 4.2.3 was placed in a thermostatically controlled oven at room temperature. The voltage across the discs for a current of 1.0 A was measured and then the oven temperature was raised slowly. Periodically it was stabilized for about 20 min, and the voltage measured. When the temperature reached about 83°C, the oven was turned off, and the discs were left inside overnight. The next morning it was noticed that the contact faces of the brass discs did not stick together, in spite of the coatings of Wood's Metal. This experiment was rerun twice.

The voltage readings for each run were plotted against the temperature in Fig. 17(a). The plot shows that the voltage slightly increased with temperature up to about 70°C, remained constant to about 72°C and then decreased, reaching a minimum at 74°C. Further increase of temperature resulted in a sharp rise of voltage. This was regarded as an indication that the high spots of the contact surfaces became exposed after the Wood's Metal was thoroughly melted and allowed to drain to the low spots.

4.2.4.2. Thick Coating

The brass discs were removed from the oven, and their surfaces recoated by a thicker layer (about 0.05 mm) of Wood's Metal. The voltage across the discs was measured at a constant current of 1.0 A as described in Sect. 4.2.4.1, while the oven temperature was raised to 93°C. This time the discs adhered to each other firmly after cooling.

The voltage readings, plotted against the temperature in Fig. 17(b), show an abrupt decrease from 0.35 mV at 65°C to about 0.02 mV at 70°C.

The above results indicate that the minimum thickness of coating prompting the adherence of the surfaces is between 0.01 and 0.05 mm.

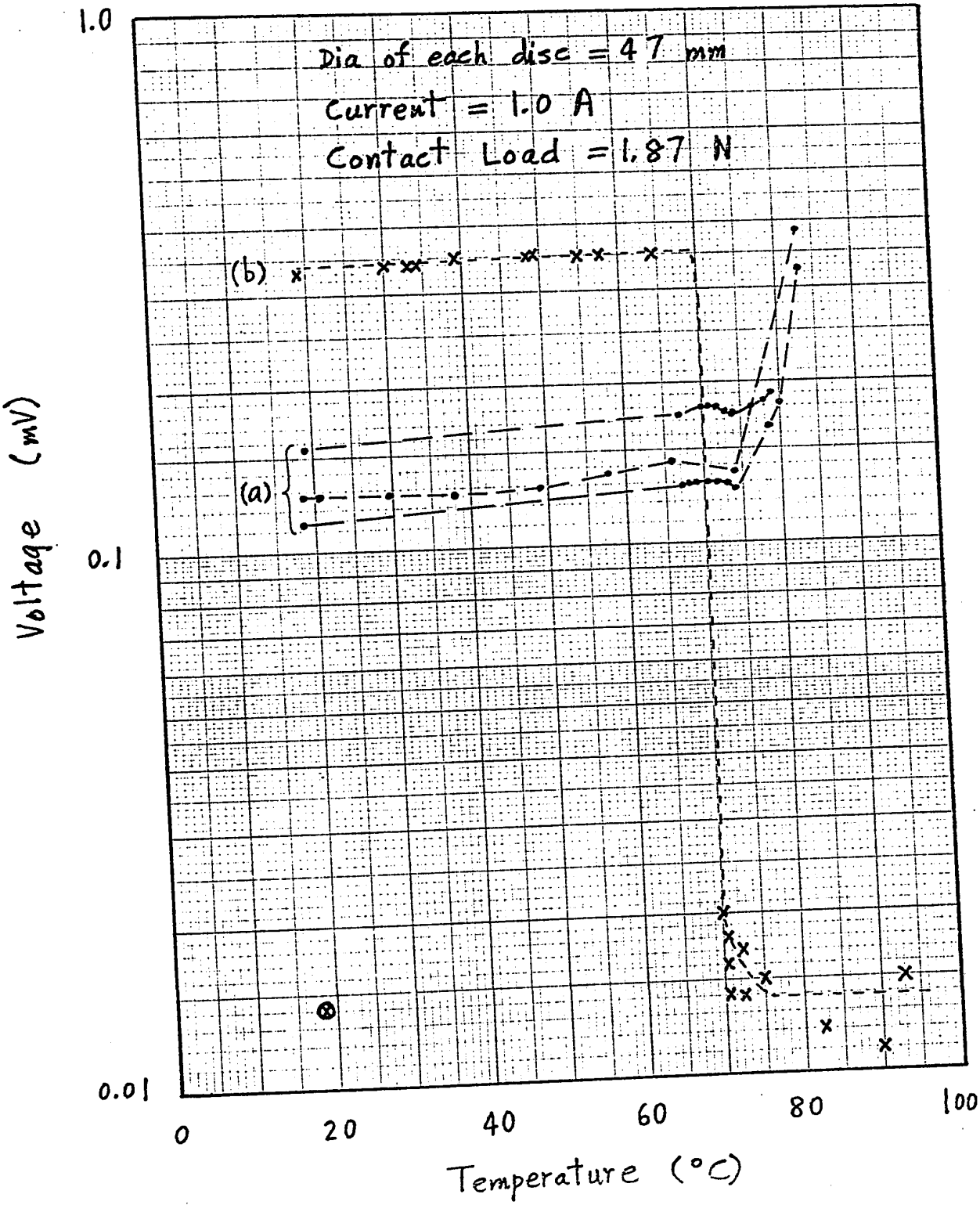

Fig. 17 : Voltage across two Contacting Brass Discs coated with Wood's Metal and at elevated Temperatures

(a), • : 0.01 mm thick coating
(b), x : 0.05 mm thick coating (⊗ : after cooling from melting)

4.3. Steel Ball to Brass Disc Contacts

4.3.1. Description of Apparatus

An apparatus* (Fig. 18) was constructed to study steel ball to brass disc contacts. A chrome-plated steel ball was placed between two brass discs of 4.7 cm diameter. The lower disc rested on a polyurethane foam pad, which was 0.3 cm thick when not compressed. This pad in turn lay on top of a cylindrical nylon block. The upper disc was permanently attached to one end of a brass shaft of 0.95 cm diameter. Using a motor and gears, the shaft could be rotated at 1.9, 5.8, or 17.4 rpm. The assembly included four nylon bushings for supporting the brass shaft in an upright position, a spring for exerting pressure on the upper disc, and a short glass tube to prevent the ball from falling outside. A current lead and a potential lead were attached to the brass shaft. Part of the shaft served as a bobbin, on which these leads were wound when it rotated. A current lead and a potential lead were also connected to the lower disc.

---

* I am grateful to Mr D. P. Kingswell for constructing this apparatus.

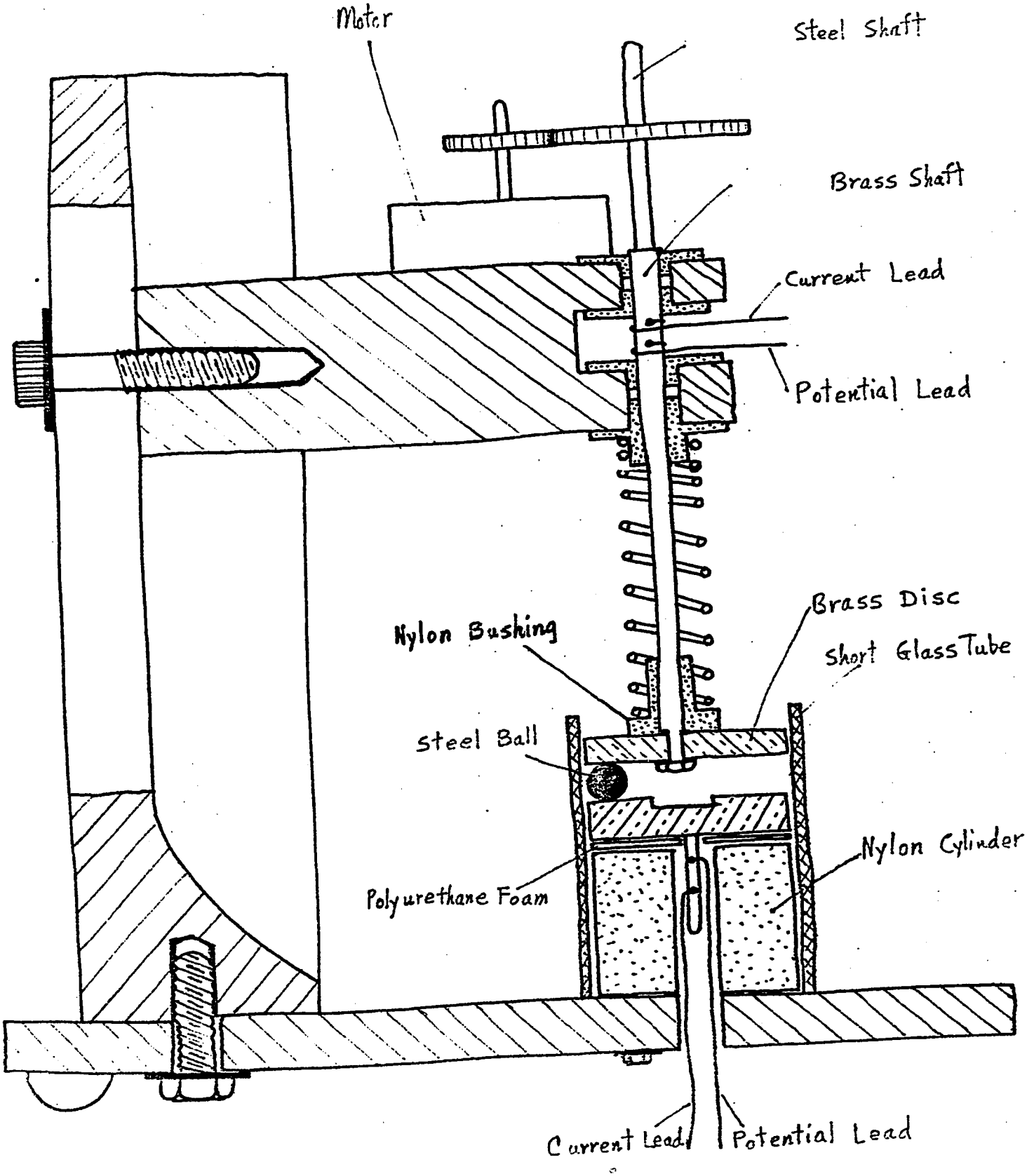

Fig. 18 : Apparatus for studying Ball-to-Disc Contact

4.3.2. Bare Brass Surfaces

4.3.2.1. Stationary Contact

The current leads of the apparatus described in Sect. 4.3.1 were connected, in series with a 5-Ω resistor, to a regulated dc power supply (Kepco CK18-3M) (Fig. 19). To eliminate the transient voltage fluctuations, an RC-integrating circuit with a time constant of 10 s was connected across the potential leads. The voltage across the capacitor of this circuit was fed to a high impedance voltmeter (Fluke 845AR) whose isolated output was connected to a chart recorder (LN Speedomax) for a continual display of the capacitor voltage.

With the shaft of the apparatus stationary and using a steel ball of 0.64 cm diameter, the current was varied in steps, and the voltage across the discs was recorded on a paper chart (Fig. 20). Since the ball was in contact with both discs, the measured voltage accounted for two ball-to-disc contacts. However, the horizontal scale of Fig. 20 was labelled in such a way that the time-voltage trace would read half the measured value to correspond to the voltage across a single contact. The contact load was mainly due to the weight of the upper disc and the shaft, and was about 1.5 N.

Fig. 20 shows that the voltage was proportional to the current while the latter was increased in 0.1 A steps from 0 to 0.3 A. Further increase of current from 0.3 to 1.0 A in the same steps, and from 1.0 to 2.0 A, resulted in progressively diminishing voltage increases. However, after this initial 2 A current, further current changes in this range (0 - 2 A) produced fairly proportional voltage changes, with a constant of proportionality different from the initial one. The change of proportionality probably indicated that the contact area had increased due to the softening of the brass when the voltage exceeded 0.16 V.

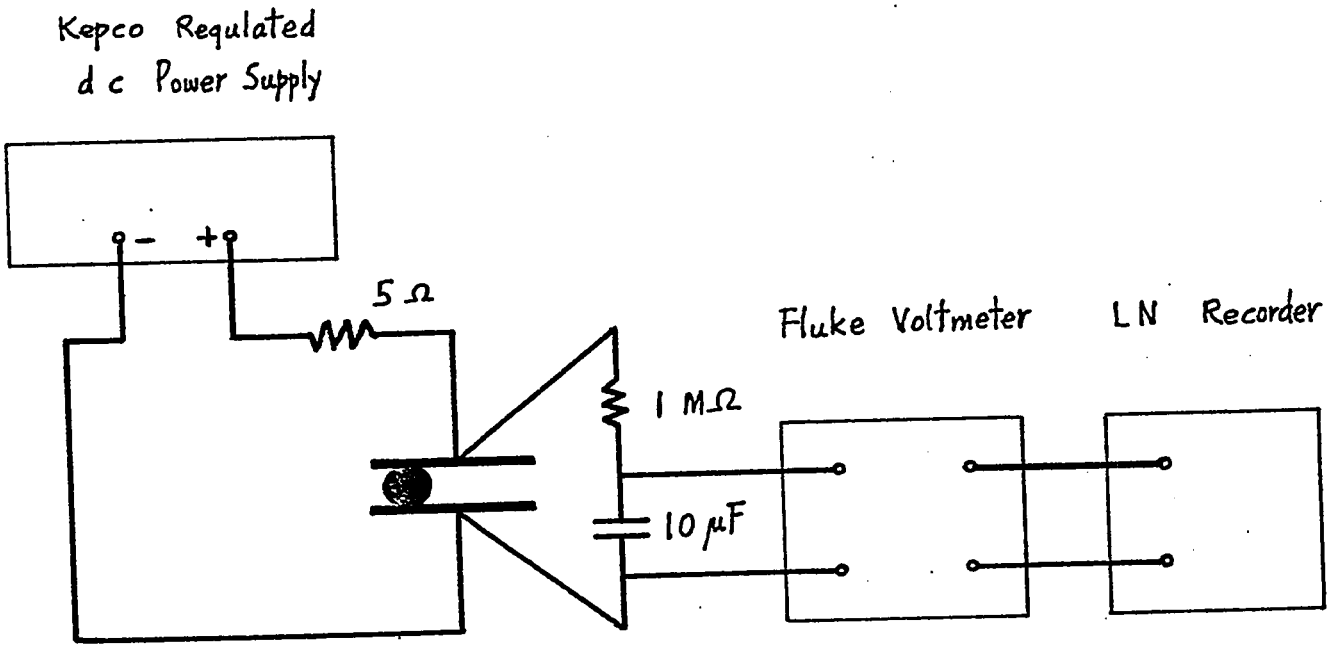

Fig. 19 : Experimental Setup for Studying Contact between Steel Ball and Brass Discs

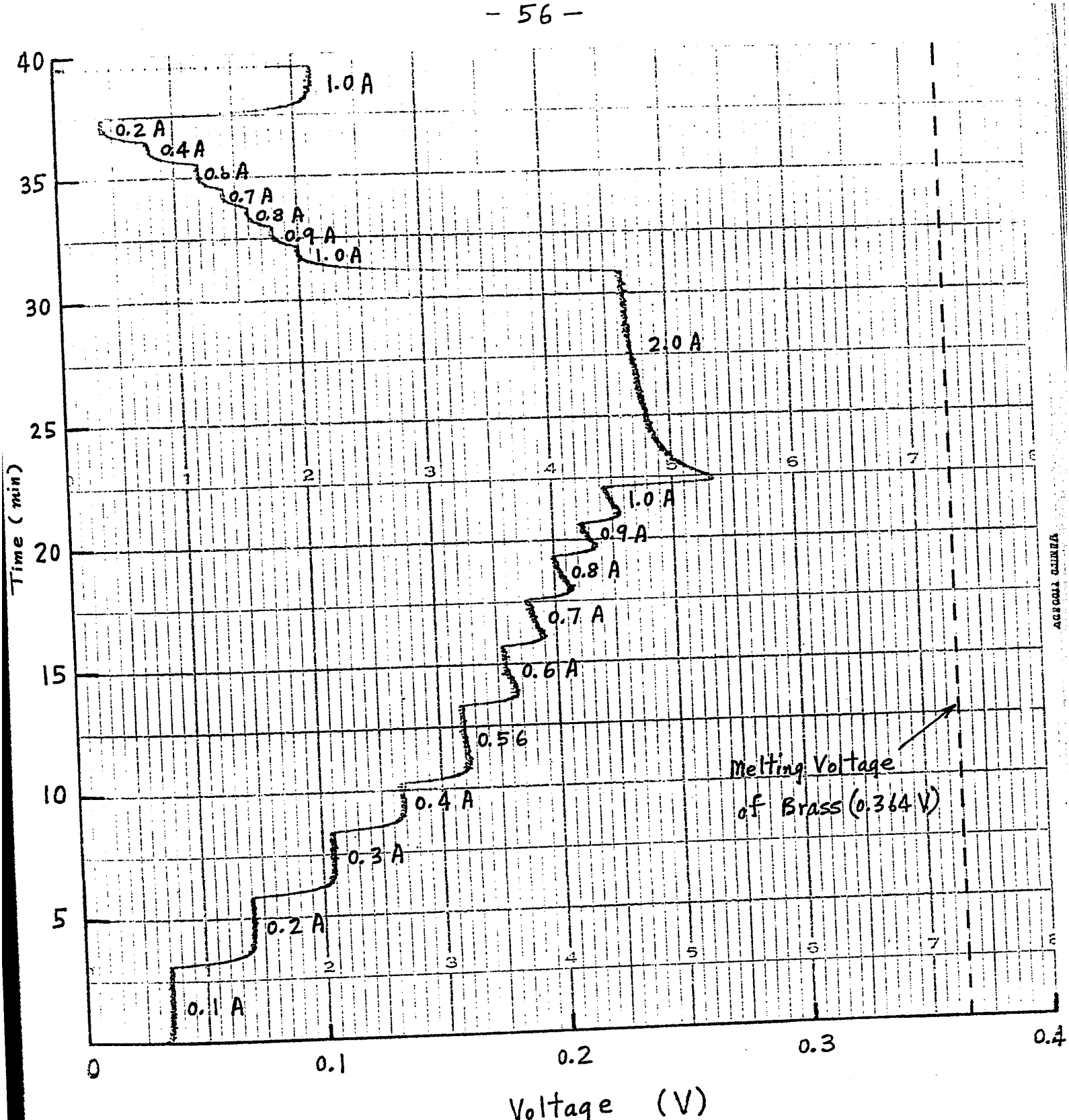

Fig. 20 : Voltage of the Stationary Contact between a Steel Ball and a Bare Brass Disc

(Dia of Ball = 6.4 mm ; Contact Load = 1.5 N)

4.3.2.2. Rolling Contacts

4.3.2.2.1. Fluctuations of Voltage at Constant Current

The rotation of the ball (0.64 cm diameter) in the apparatus described in Sect. 4.3.1 caused fluctuations of the voltage across the discs even at constant current. At first the quality of the current regulation of the power supply was investigated, using the experimental setup shown in Fig. 21a. With the shaft stationary and the current at 0.2 A, the current trace was displayed on an oscilloscope (Tektronix Type 555) and photographically recorded as shown in Fig. 22a. Without adjusting the power supply, the shaft was rotated, causing the ball to roll. Again a current trace was recorded on the same picture. With the power supply off and the shaft stationary, a zero current trace was recorded for reference.

Using the experimental setup as shown in Fig. 21b, the voltage across the two brass discs was now displayed on the oscilloscope. The voltage traces were recorded as before and are shown in Fig. 22b.

The current traces in Fig. 22a show that the current in the rolling case was lower than in the stationary case by approximately 3%, but it did not fluctuate. However, the voltage in the rolling case fluctuated and was higher than in the stationary case, as shown in Fig. 22b. In terms of resistance, this means that the resistance of the rolling contact was higher than that of a stationary one.

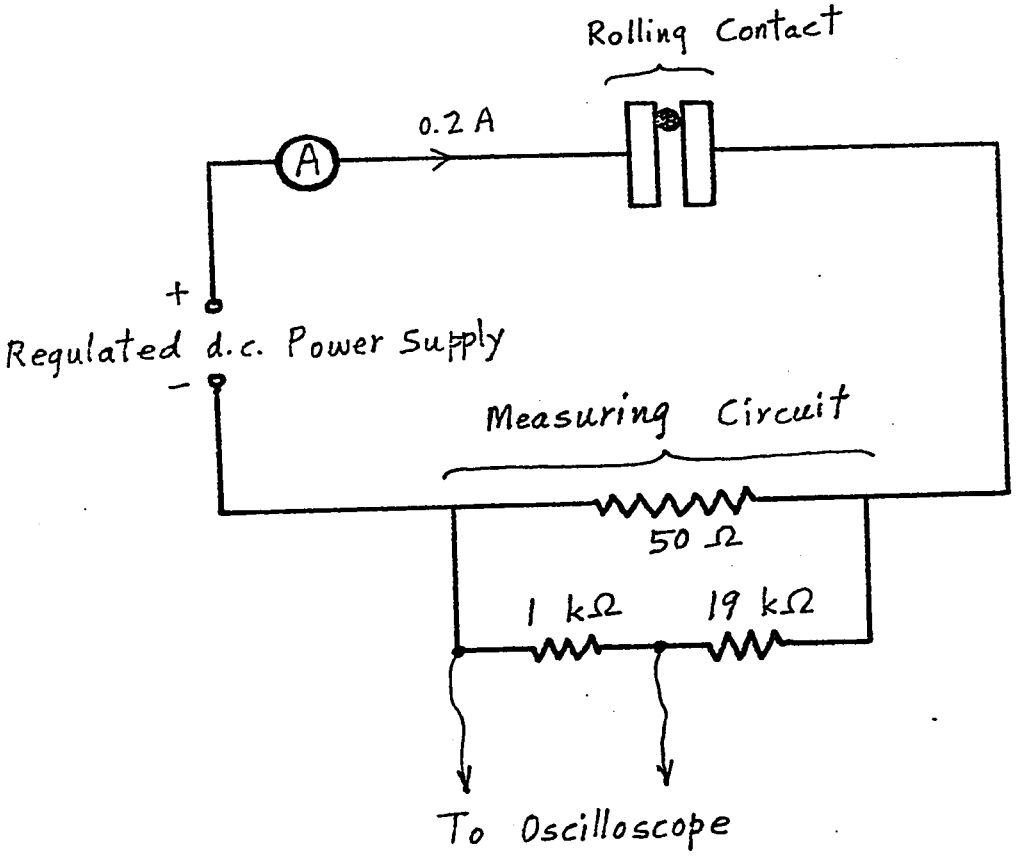

Fig. 21 a: Circuit for Current Display

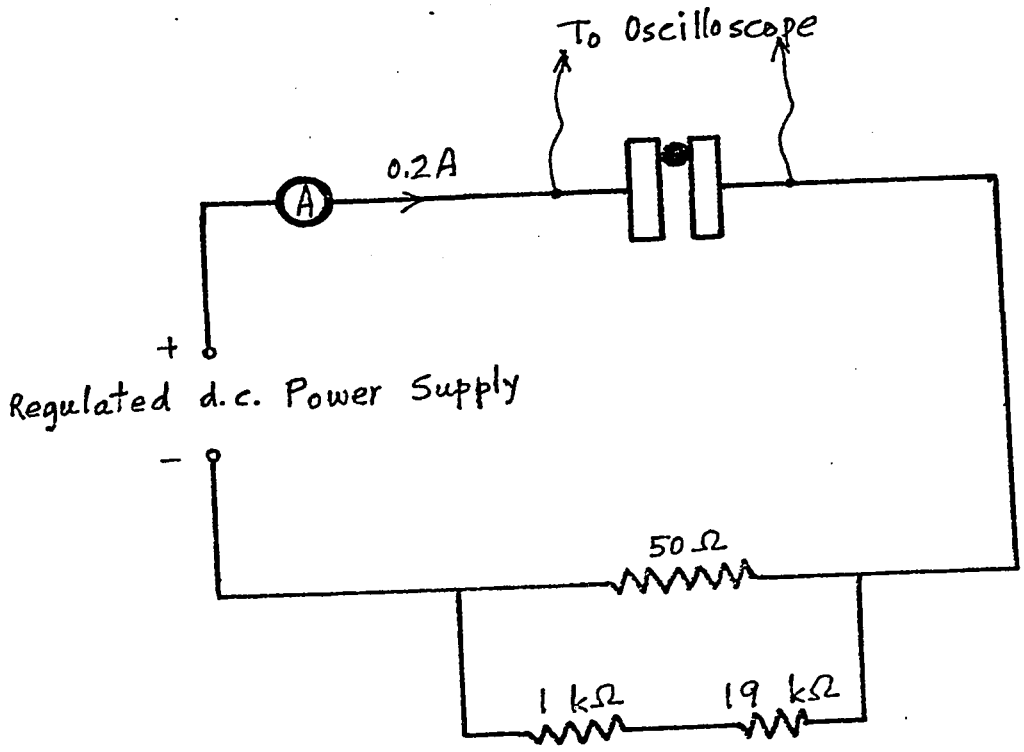

Fig. 21 b: Circuit for Voltage Display

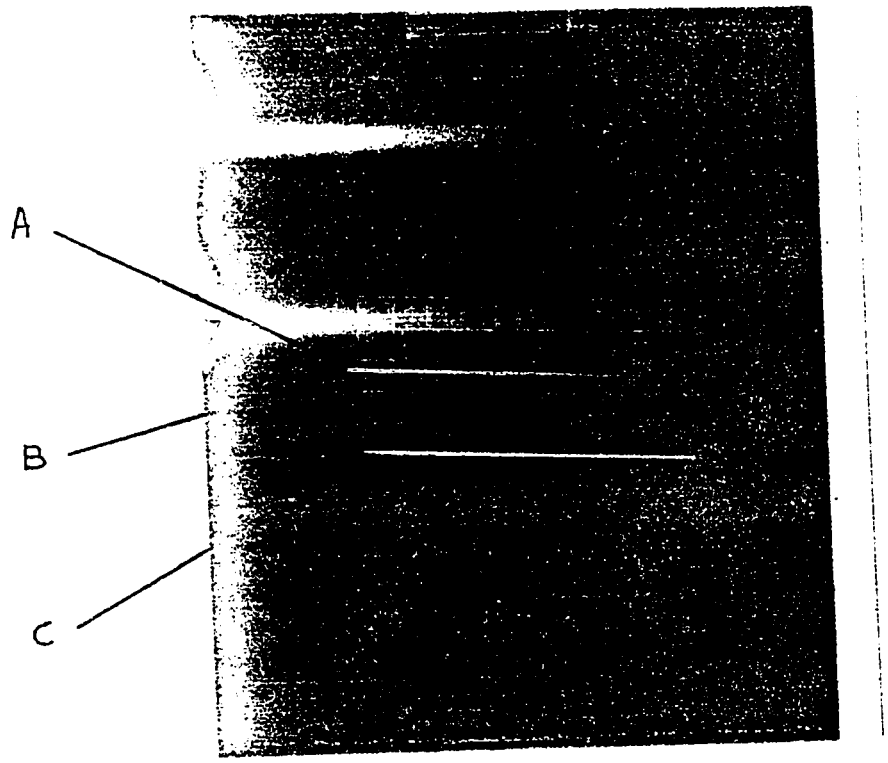

Fig. 22 a : Three Traces showing Current through two Brass Discs with a Steel Ball between them

Dia of Ball : 0.64 cm

Vertical Scale : 0.2 V/cm

Horizontal Scale : 2 ms/cm

Traces from top to bottom

A : 0.2 A and Stationary

B : 0.2 A and Rolling (Shaft Speed : 1.93 rpm)

C : 0 A and Stationary

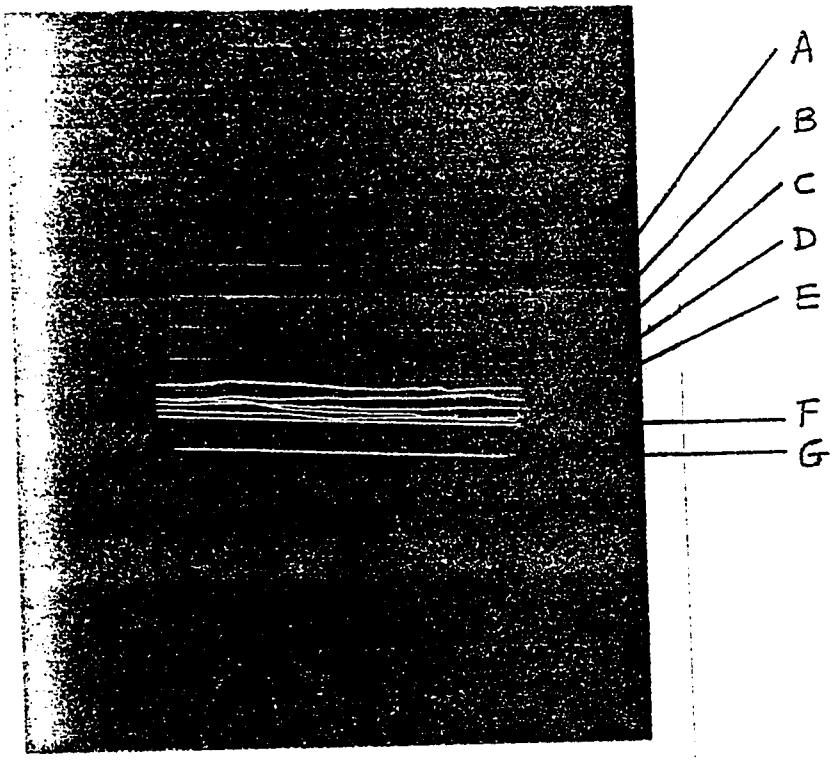

Fig 22b : Seven Traces showing Voltage across Two Brass Discs with a Steel Balls between them

Dia of Ball : 0.64 cm

Vertical Scale : 0.2 V/cm

Horizontal Scale : 2 ms/cm

Traces from top to bottom

A, B, C, D, E : 0.2 A and Rolling (Shaft Speed : 1.93 rpm)

F : 0.2 A and Stationary

G : 0 A and Stationary

4.3.2.2.2. Dependence of Voltage on Current and Speed

Using the apparatus and the experimental setup as shown in Figs. 18 and 19 respectively, the voltage across the brass discs was measured while the current was varied from 0.1 to 1.0 A with the ball rolling. Steel balls of four different sizes were used, their diameters being 0.16, 0.32, 0.48, and 0.64 cm respectively. The shaft speeds used were 1.9, 5.8, and 17.4 rpm.

Fig. 23 shows the voltage-current characteristics for balls of the four sizes. In general, the voltage increased with current up to about 0.7 A, and then levelled off with further increase of current. A superficial examination of the experimental data showed no systematic correlation between the voltage and the shaft speed. However, the results indicate that, other conditions being equal, the use of a larger ball resulted in a lower voltage drop across the brass discs. This agrees with the intuitive reasoning that a larger ball would have a larger contact area with the discs, and thus a smaller contact resistance.

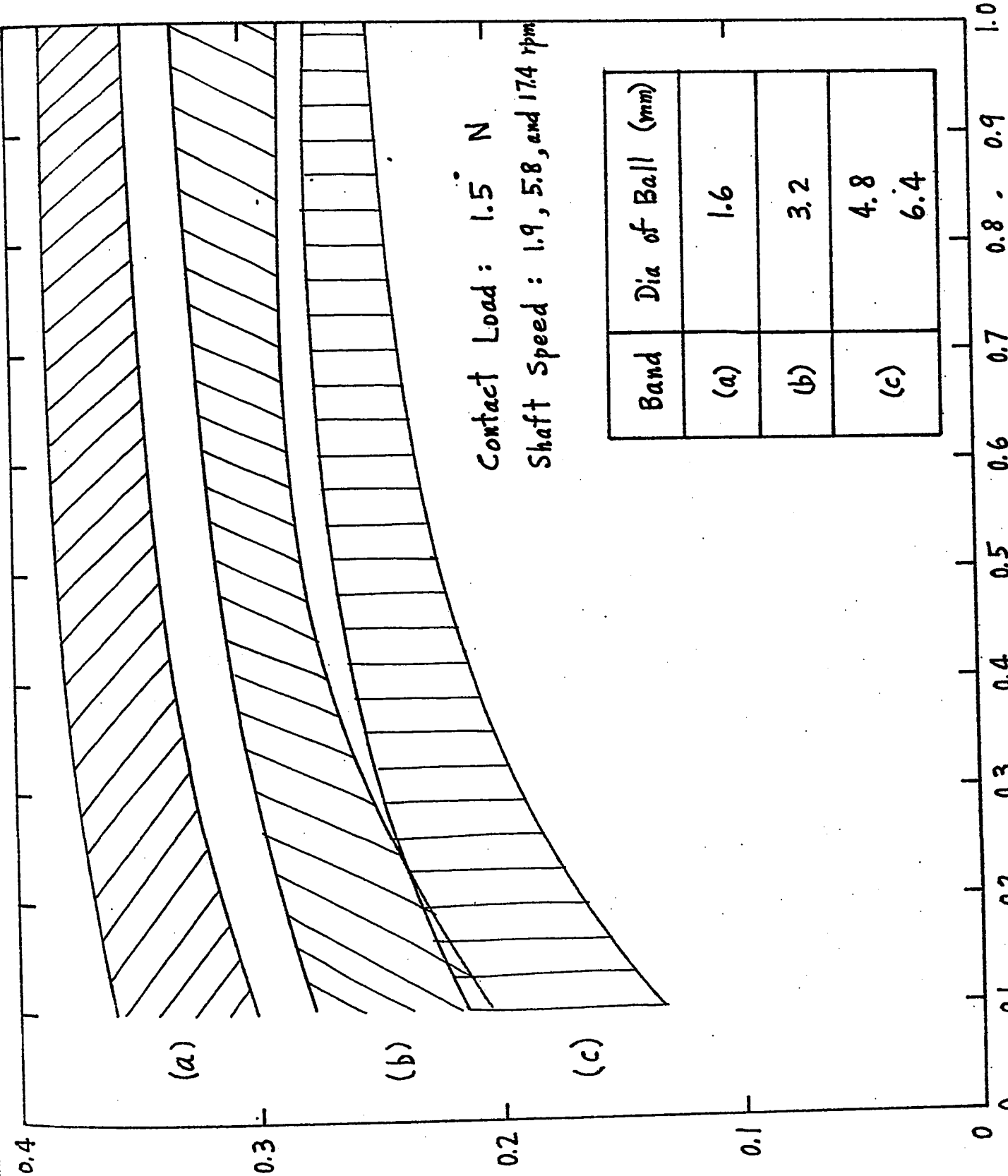

Fig. 23 : Voltage-Current characteristic of the Contact between a Rolling Steel Ball and a Bare Brass Surface

4.3.3. Surfaces coated with Wood's Metal

4.3.3.1. Stationary Contact

Each of the two brass surfaces in contact with the steel ball in the apparatus shown in Fig. 18 was coated with a layer of Wood's Metal about 0.05 mm thick. Using a steel ball of 6.4 mm diameter, an experiment similar to that described in Sect. 4.3.2.1 was performed. The corresponding chart record is shown in Fig. 24.

In the current range between 0.1 and 1.0 A, the voltage fluctuated violently about a value that remained more or less constant independent of the current. This was regarded as an indication that the Wood's Metal at the points of contact was melted by the heat produced by the current. It was observed that the voltage was proportional to the current when the latter was below 0.02 A.

4.3.3.2. Rolling Contact

With the shaft rotating at 17.4 rpm and using the same steel ball as in Sect. 4.3.3.1, the voltage across the brass discs was measured at various currents as described in Sect. 4.3.2.2.2. This experiment was repeated with a coating of Wood's Metal about 0.01 mm thick.

Fig. 25 shows the voltage-current characteristics for the two cases. In general, the characteristic corresponding to the thicker coating lies below the one corresponding to the thinner coating, showing that the contact resistance was lower in the former case.

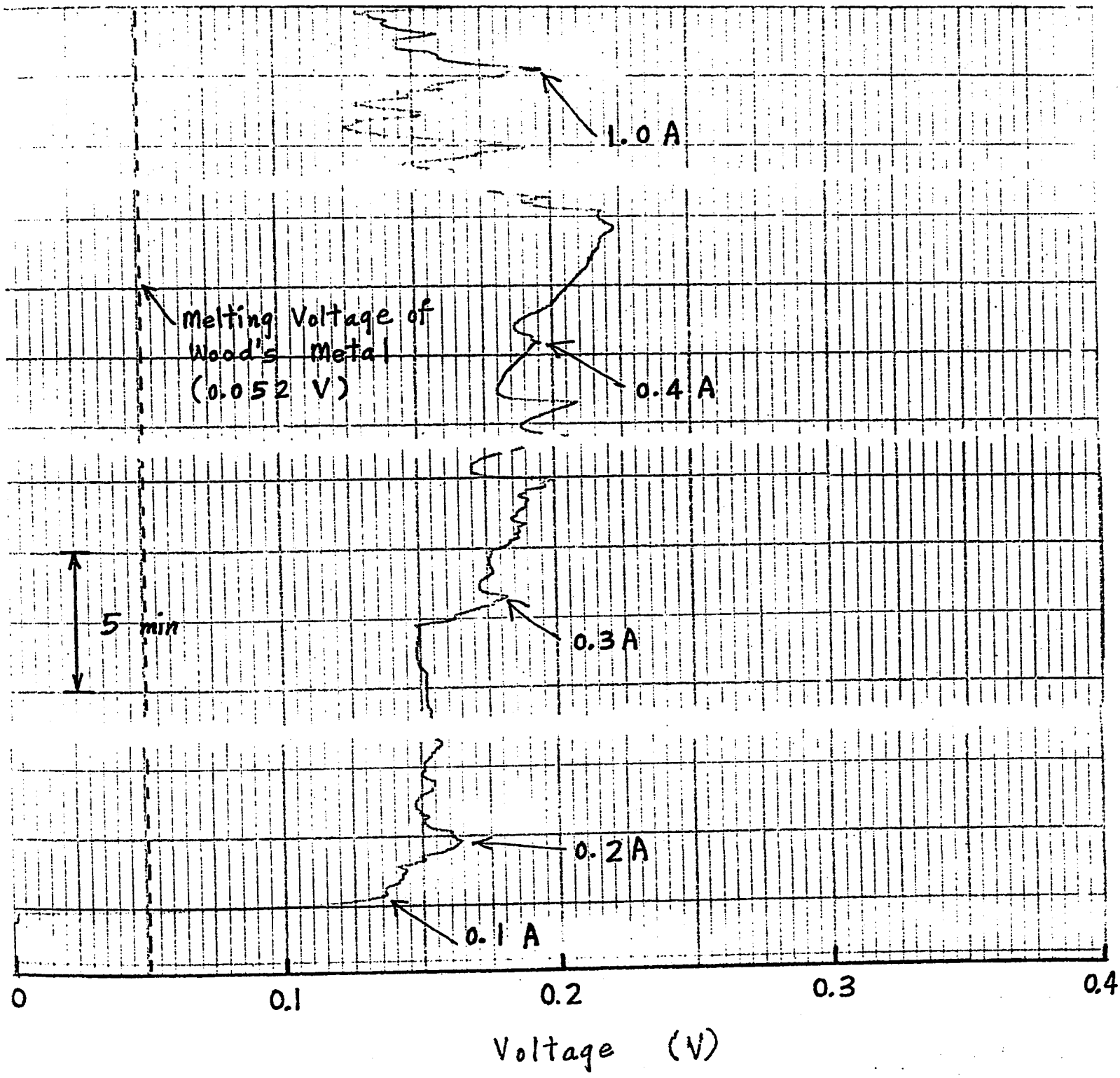

Fig. 24 : Voltage of the Stationary Contact between a Steel Ball and a Brass Disc coated with Wood's Metal about 0.05 mm thick (Dia of Ball = 6.4 mm ; Contact Load = 1.5 N)

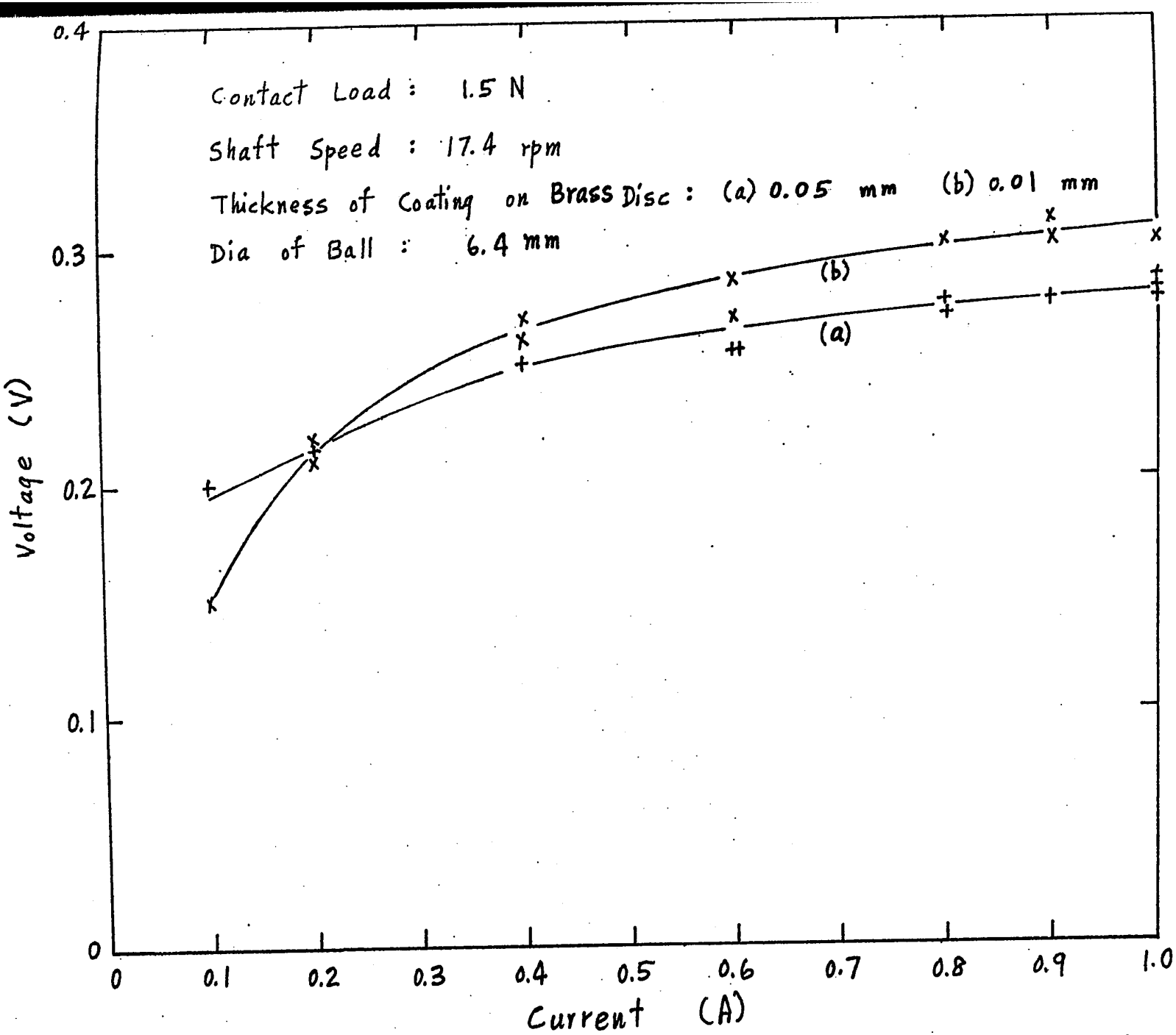

Fig. 25 : Voltage-Current Characteristics of the Contact between a Rolling Steel Ball and a Brass Surface coated with Wood's Metal

4.4. Rolling-Contact Current Collectors

4.4.1. Ball Bearings as Current Collectors

Three commercially available ball bearings were spaced approximately 7.6 cm from centre to centre along a common brass shaft of 1.27 cm diameter (Fig. 26), and mounted on brass supports to which current and potential leads were connected. Each bearing had eight steel balls of 0.32 cm diameter, 1.27 cm bore, and 2.86 cm outside diameter. With the shaft rotating at 360 rpm and carrying no external load, two of the current leads were connected to a regulated dc power supply (Sorensen DCR20-250A). The current was varied from 10 to 100 A in steps of 10 A, and from 100 to 250 A in steps of 50 A. The voltage across the corresponding pair of bearings was noted in each step. Similarly, voltage and current readings were obtained for each of the two remaining pairs of bearings.

For a particular current I, the voltages V_a, V_b, and V_c, across the three bearings were obtained by solving the simultaneous equations,

$$V_a + V_b = V_{ab}$$

$$V_b + V_c = V_{bc}$$

$$V_c + V_a = V_{ca}$$

where V_{ab}, V_{bc}, and V_{ca} were the voltages across the pairs of bearings. By plotting the voltages across the individual bearings, and by repeating the procedures for the other currents, the voltage-current characteristics for the bearings were obtained. These characreristics were similar to one another, and one of them is shown in Fig. 27(a). It shows that the voltage slowly increased from about 0.7 V at 10 A to less than 1 V at 250 A. Since the balls made contact with both the inner and the outer races, the voltage as plotted accounted for two contact interfaces electrically in series. Therefore, the voltage per contact interface varied from 0.3 to 0.5 V,

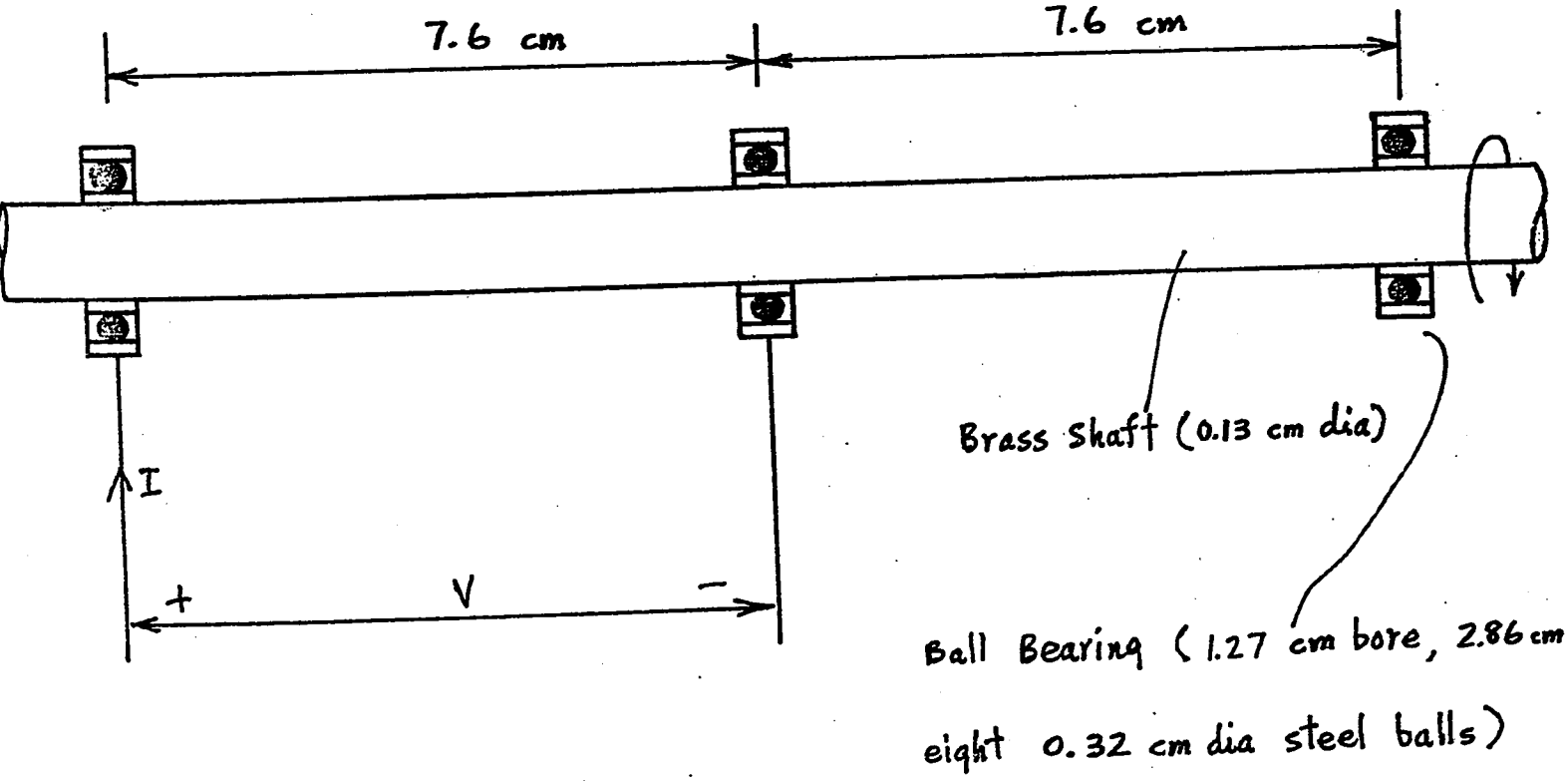

Fig. 26: Experimental Setup for Measuring Voltage Drops of Ball Bearings

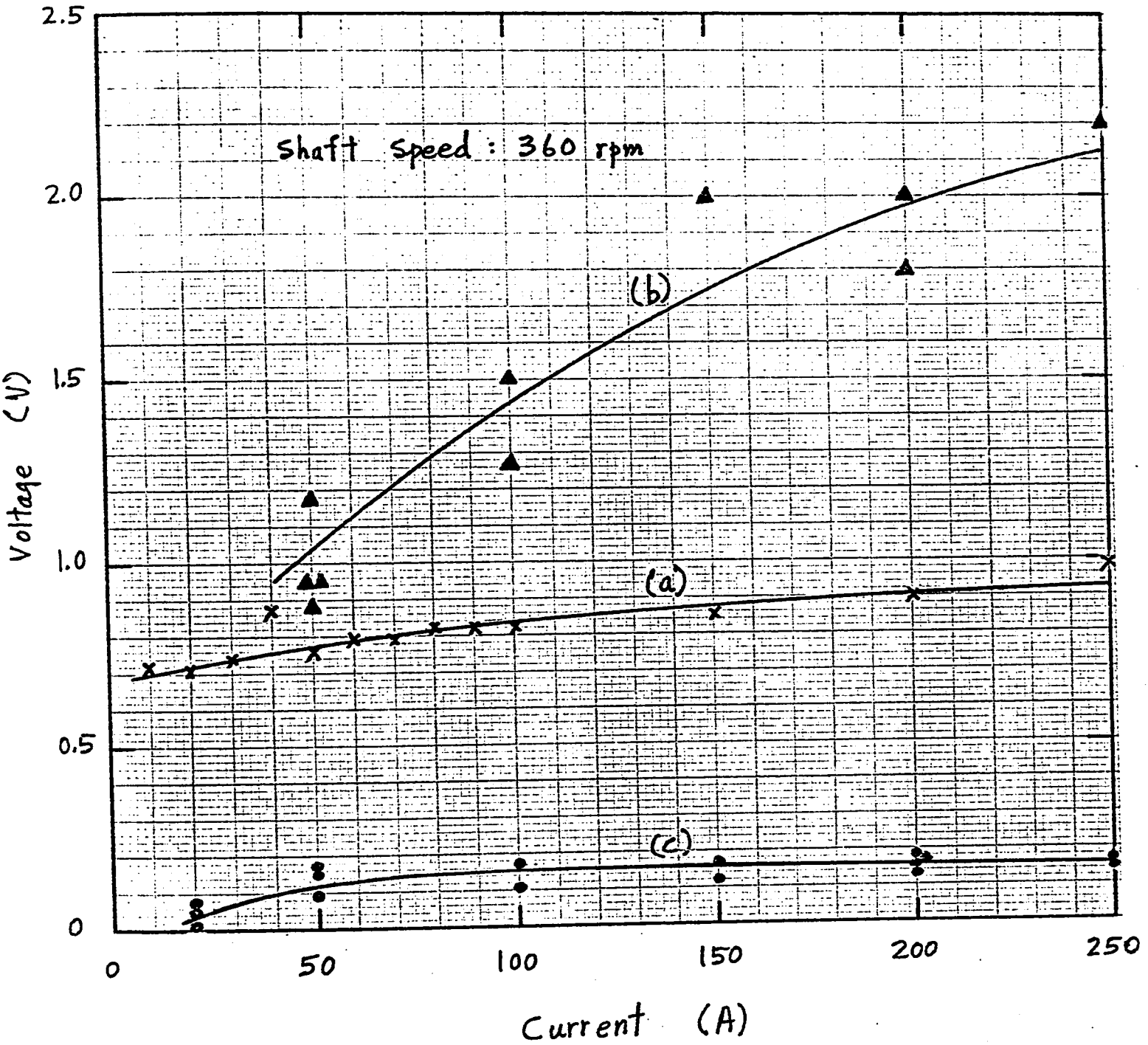

Fig. 27 : Voltage-Current Characteristics of Three Rolling-Contact Current Collectors

(a), X : Commercial Ball Bearing (1.27 cm bore, 2.86 cm od, eight 0.32 cm dia steel balls)

(b), ▲ : Experimental Current Collector with Bare Brass Contact Surfaces (Details shown in Fig. 28)

(c), ● : Above Current Collector with Contact Surfaces coated with Wood's Metal

and did not exceed the melting voltage of steel (0.52 V).

The balls and races of a similar ball bearing were wetted by the liquid metal, GaIn. However, because of the close tolerances in manufacture, the balls failed to roll in their races after wetting. This failure prompted the construction of the experimental current collectors described in the next two sections.

4.4.2. Experimental Current Collector wetted by GaIn

An experimental current collector of the form shown in Fig. 28 was constructed. Steel balls and aluminum discs were used, and the grooved tracks and balls were wetted by GaIn, which is liquid at room temperature. An attempt was made to measure the voltage across the outer discs at various currents. However, because of the heat generated by the current, the liquid metal degraded rapidly and also attacked the aluminum discs. Therefore, this experiment was discontinued.

4.4.3. Experimental Current Collector Wetted by Liquid Wood's Metal

The experimental current collector shown in Fig. 28 was made of three coaxial brass discs. The opposing faces of the discs had pairs of V-grooved circular tracks of 2.54 cm diameter, each pair accommodating twenty five steel balls of 0.32 cm diameter. Initially, the tracks were bare brass. With the inner disc rotating at 360 rpm, the outer discs were held stationary and connected to the power supply (Sorensen DCR20-250A). The voltage across the outer discs was measured while the current was increased stepwise from 50 to 250 A. The voltage readings corresponding to these various currents are plotted in Fig. 27(b).

An ample amount of Wood's Metal was then melted in each track, and allowed to drain away under gravity. The voltage readings of the resulting liquid-metal-wetted* collector for various currents were similarly obtained, and plotted in Fig. 27(c).

The results show that the presence of liquid Wood's Metal reduced the voltage drop across the two outer discs to less than 0.2 V for currents up to 250 A. This voltage drop accounted for four contact interfaces electrically in series, because there were two sets of balls, one on each side of the inner disc. Therefore, the voltage drop per contact interface was less than 0.05 V. and did not exceed the melting voltage of Wood's Metal.

This experiment seemed to be very promising, and therefore further work towards its improvement should follow. However, it would probably be better to carry out such work in another research project, due to the time limitation for the submission of this thesis.

---

* The heat produced by the current was sufficient to maintain the Wood's Metal in the molten state, and it was not necessary to heat the current collector thermally.

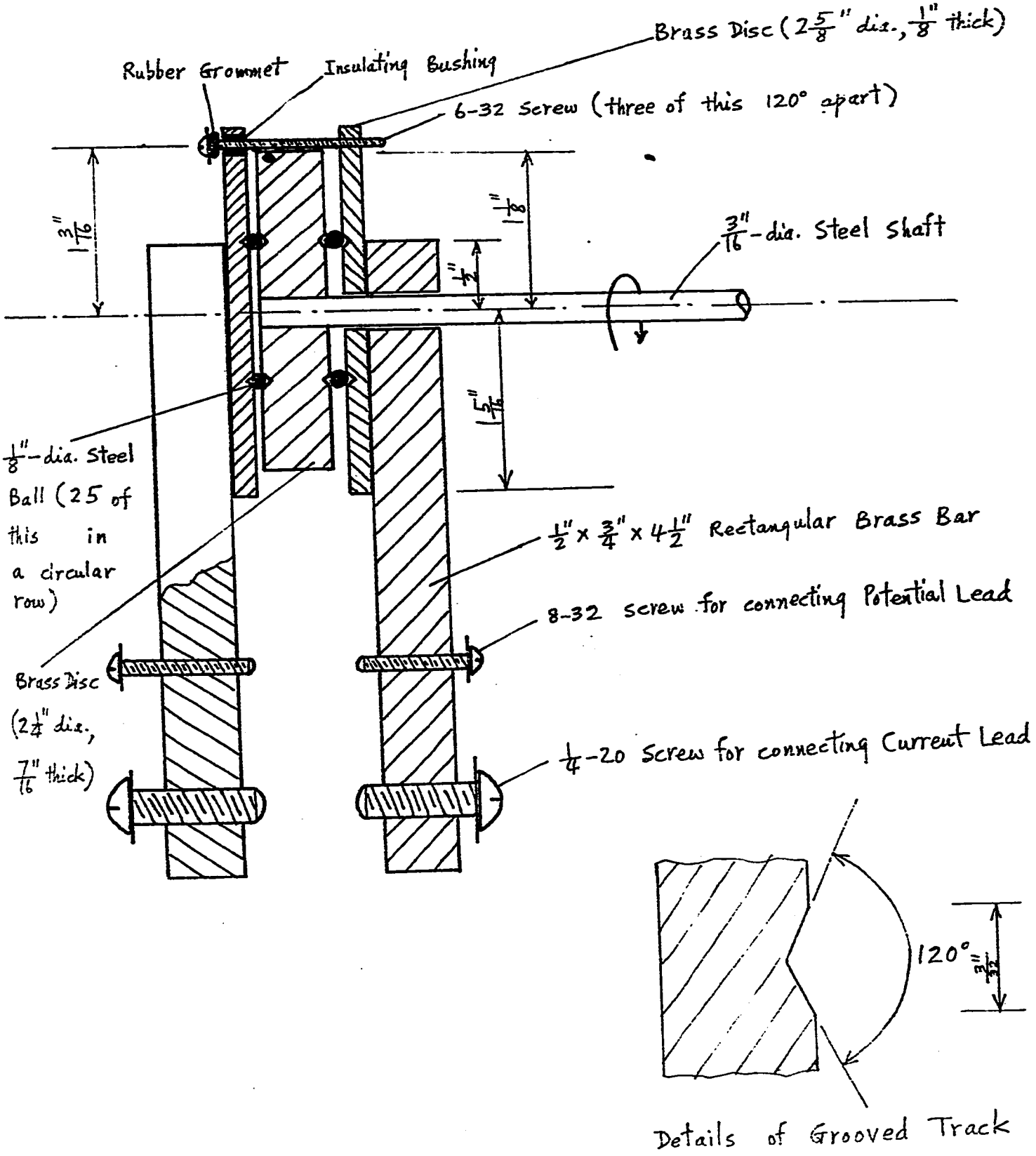

Fig. 28 : The Experimental Rolling-Contact Current Collector

V. Summary and Conclusion

The problems arising from current collection in electric motors and generators have existed since the invention of the first rotary electric machine, i.e. since about 1831 when Michael Faraday generated electricity by mechanically rotating a metal disc in a magnetic field.

These problems originated from the necessity of transferring a current across the contact interface between two electrical conductors moving with respect to one another. Such a relative motion produces a number of undesirable phenomena: a voltage drop across the interface; bouncing of contacts, and the accompanying arcing; mechanical wear and tear, and the resulting frictional loss. No satisfactory solution to all of these problems has been found.

The most commonly used current collection systems employ carbon, or metal-impregnated carbon brushes. They suffer from relatively high voltage drops, and are unsuitable for homopolar motors. The work on this thesis was an attempt to solve the current collection problem in homopolar motors, particular for automobile propulsion, by using liquid-metal-wetted rolling-contact current collectors.

To the author's knowledge, such collectors have not been mentioned in the literature. Because of this lack of references to previous work, the investigation here had to begin with the elementary cases.

In the first place, the electrical properties of stationary contacts between two bare brass surfaces, and then between two brass surfaces coated with Wood's Metal, were investigated. The presence of Wood's Metal significantly reduced the voltage drop across the contact interface, by about an order of magnitude.

Secondly, slow-speed (up to 17.4 rpm) rolling contacts between surfaces, both bare and coated, at room temperature were investigated for small currents (up to 1 A). The results indicated that a layer of Wood's

Metal, initially about 0.05 mm thick, did not reduce the voltage drop, probably because such a layer was insufficiently thick and the high spots of the contact surfaces became exposed after running in. Further experiments should be performed with thicker layers, and at temperatures above the melting point of Wood's Metal.

Finally, higher speed (360 rpm) rolling-contact current collectors carrying larger currents (up to 250 A) were investigated, using bare surfaces and also surfaces wetted heavily* by liquid Wood's Metal. The results for the wetted case showed that the voltage drop per contact interface was less than 0.05 V. This is promising, and therefore further experiments might be worthwhile, such as measuring the voltage drop at higher speeds up to about 10 000 rpm, at which a homopolar motor is expected to operate.

In addition to the experimental investigation, theoretical analysis of three fundamental aspects was presented. The first part of this analysis showed that, for a given size of rolling-contact current collector, the total contact area resulting from using small balls is greater than from using large balls. The second part showed the existence of electrodynamic forces, due to the currents being constricted at the contact spots, tending to separate the contact surfaces. If the currents through the constrictions are sufficiently large, the accompanying electrodynamic forces will be large enough to nullify the contact load and thus separate the contact, resulting in the bouncing of the contact surfaces. The presence of liquid metal reduces the magnitude of the current constriction by increasing the actual contact areas at the contact spots, thus reducing the electrodynamic forces. This should be investigated further both theoretically and experimentally.

---

* The layers of liquid Wood's Metal were as thick as what could be by adhesion and under gravity.

The last part showed the rise of temperature at the contact interface, due to the Joule heating effect, as a function of the voltage drop across the contact members. For Wood's Metal, the heat generated by the current corresponding to a voltage drop of only 0.052 V is sufficient to cause melting to occur at the contact interface. It seems necessary to circulate oil for heat removal. This should not be regarded as a serious drawback, because the heat removed can be utilized in several ways, for example, defrosting the windshield of the electric automobile. In addition, the oil will prevent the contact surfaces from degrading through oxidation, and can serve as an agent both for melting the Wood's Metal when starting the motor, and for lubricating the rolling parts when it is running.

To sum up, the results of the work of this thesis indicate that further research on the liquid-metal-wetted rolling-contact current collectors seems to be warranted. Such research should explore the effects of speed, choice of liquid metal, possible improvement by wetting the contact surfaces heavily by circulating a liquid metal, and the effects of the use of oil.

This thesis should be regarded as a starting point, rather than the completion, of the investigation of the liquid-metal-wetted rolling-contact current collectors. A complete investigation is far beyond the scope of this work, but it is hoped that it will be continued in other theses work.

Appendix A. Electrodynamic Repulsion due to Current Constriction

This problem was first studied by Dwight (42) by considering the interaction of the current in a constriction with its own magnetic field. Bron treated the problem differently by considering the magnetic pressure arising from a magnetic field (49). His analysis is presented below.

When there is a magnetic induction B existing in a medium, we can construct, at any point of the medium, a system of stresses that lead to correct explanations for the known experimental findings concerning magnetic induction. This is due to Maxwell (48). In an isotropic magnetic medium, such as free space or air, in which the magnetizing force H and the magnetic induction B are parallel and the permeability is a scalar, the stress system becomes simply a compression perpendicular to, and a tension along, the lines of force, both of magnitude $\frac{B^2}{2\mu}$ (Fig. 29). This compression is called the "magnetic pressure", and will be used to derive an expression corresponding to Dwight's [Eq. (3.6)].

Consider a conductor composed of two cylindrical portions having radii r_1 and r_2 respectively (Fig. 30). The plane that bisects these two portions will be referred to as the plane of transition. Let us picture three surfaces. Adjacent to one side of the transition plane is a circular surface S_2 belonging to that portion having radius r_2. Adjacent to the other side of the transition plane are two surfaces: a circular surface S_1, belonging to that portion having radius r_1, and a fictitious annulus S' of radii r_1 and r_2. S' is considered as belonging to neither of the two portions. We will find the force on each of these three surfaces due to the appropriate magnetic pressure. If we assume uniform current distribution and apply Ampere's law in circuital form, the magnetic induction at a point on surface S_1 at a distance r from the axis is

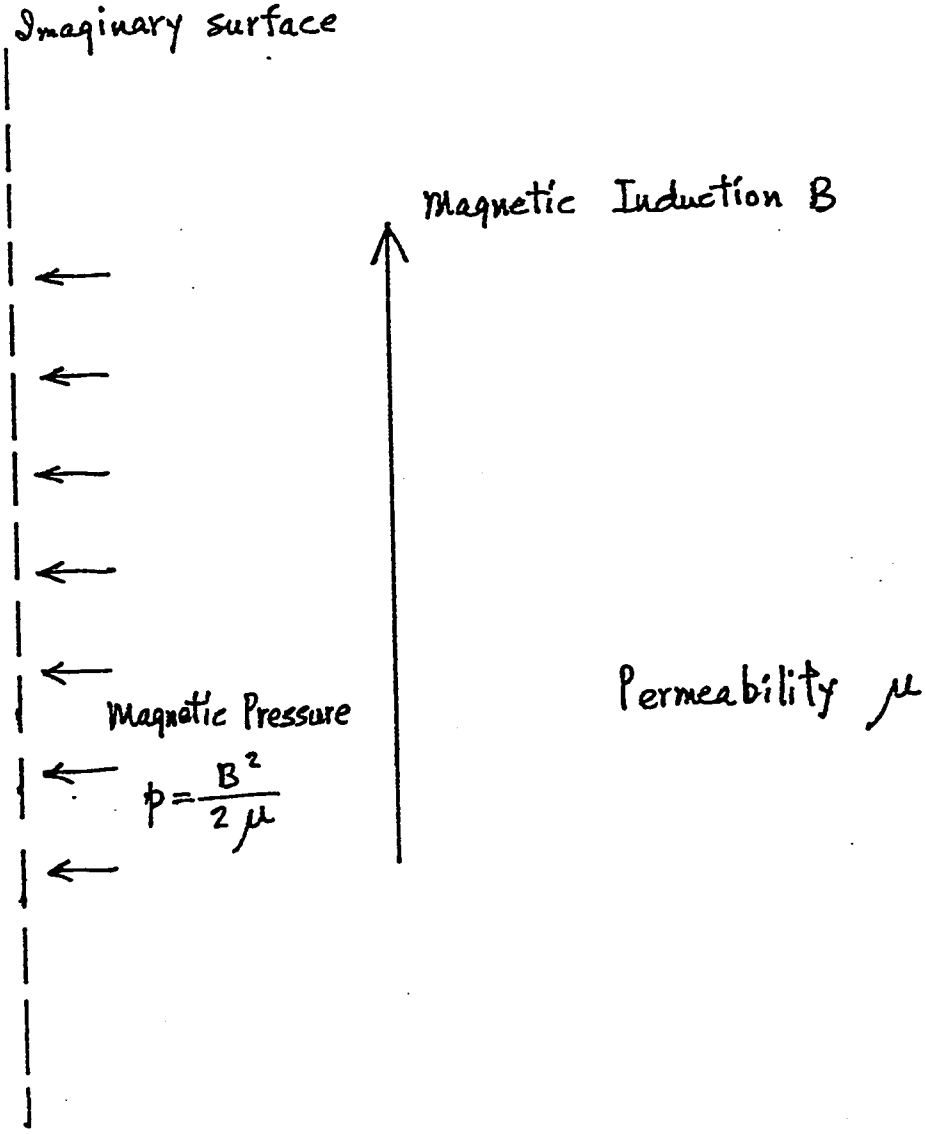

Fig. 29: The Magnetic Pressure due to the Presence of Magnetic Induction

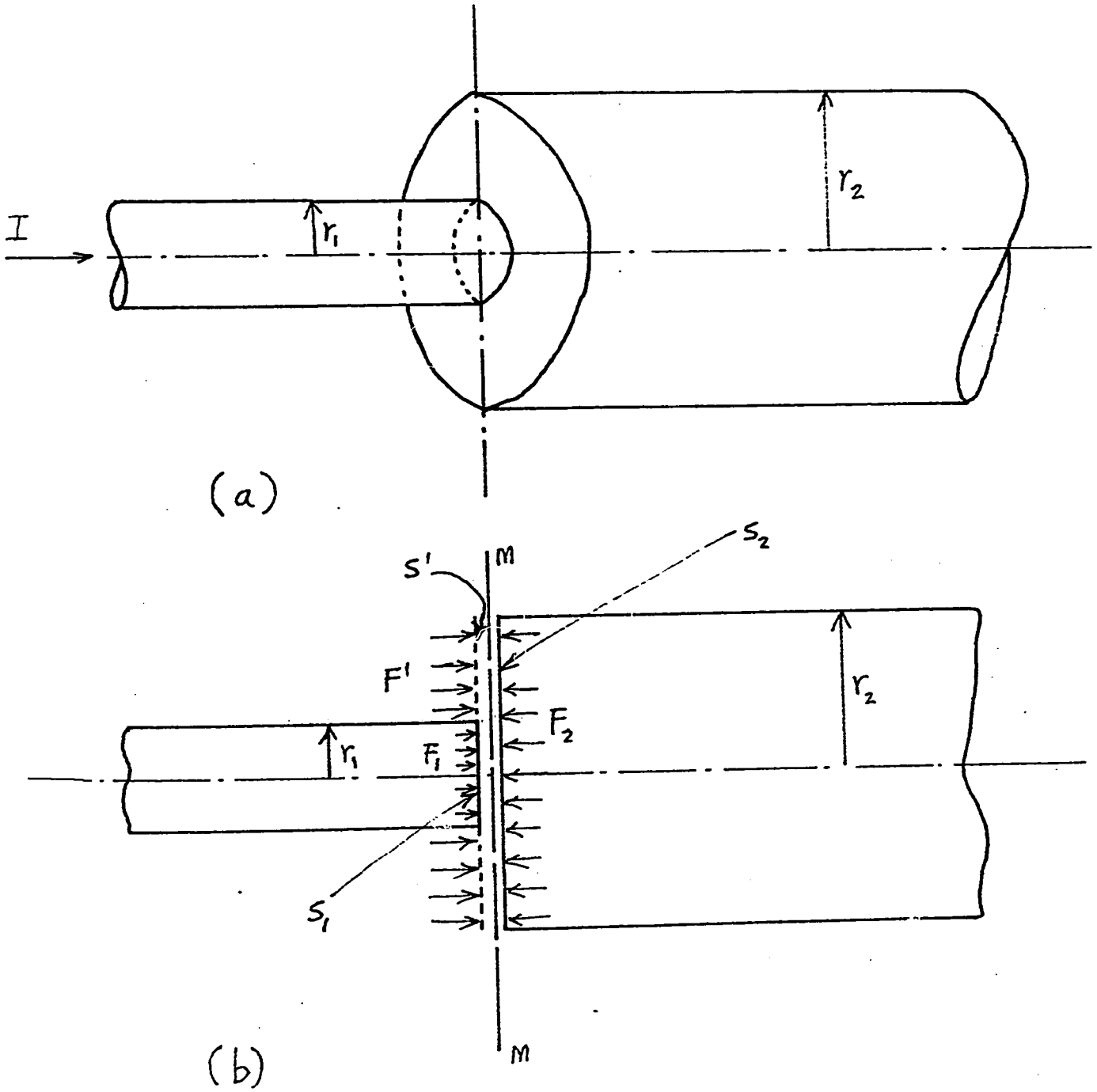

Fig. 30: A Conductor composed of Two Cylindrical Portions of Different Radii

$$B_r = \frac{\mu I r}{2 \pi r_1^2}$$

where μ is the permeability of the conductor, and I is the total current it carries. The magnetic pressure at this point is

$$\frac{B_r^2}{2 \mu} = \frac{\mu I^2 r^2}{8 \pi^2 r_1^4}$$

The force on an elementary annulus of area $ds = 2 \pi r \, dr$ and radii r and $r + dr$ is

$$dF_1 = \frac{\mu I^2 r^3}{4 \pi r_1^4} dr$$

The total force on surface S_1 is

$$F_1 = \int_0^{r_1} dF_1 = \frac{\mu I^2}{16 \pi}$$

Since this is not a function of the radius of the conductor, the force F_2 acting on the surface S_2 will be of the same magnitude as F_1. They act in opposite directions, and cancel each other. Similar reasoning will show that, for $r > r_2$, equal and opposite forces act on both sides of the transition plane, and the net force on this plane is determined solely by the force F' acting on the annulus S'.

$$F' = \int_{r_1}^{r_2} \frac{B_r'^2}{2 \mu'} 2 \pi r \, dr = \frac{\mu' I^2}{4 \pi} \ln \frac{r_2}{r_1}$$

where μ' is the permeability of the medium surrounding that part of the conductor where the radius changes. It can be shown that F' does not depend on the shape of the transition (49).

The last expression is not the same as Dwight's, because Dwight's expression contains the permeability 'μ' of the conductor. If the conductor

is of non-magnetic material and the medium is air, μ and μ' are numerically very close. In that case, either expression would give practically the same numerically value. However, in the case of a magnetic conductor, the two expression will lead to different results.

Appendix B. Resistivity of Wood's Metal

The apparatus shown in Fig. 31 was immersed in a temperature-controlled water bath. With the current through the specimen of Wood's Metal kept at 1.0 A, the voltage across the two potential terminals was measured while the temperature of the bath was slowly increased from the ice point to 90°C. The voltage readings were plotted against the temperature (Fig. 32). The resistivity ρ of the specimen at a certain temperature is given by the equation,

$$\rho = \frac{R\,A}{\ell}$$

where R, A, and ℓ are the resistance, cross-sectional area, and length of the specimen respectively. The resistivities at 20°C, 60°C, 70°C, 80°C, and 90°C were computed and are tabulated in the following table:

Temperature (°C)	Resistivity (μΩ cm)
20	43
60	48
70	50
80	95
90	98

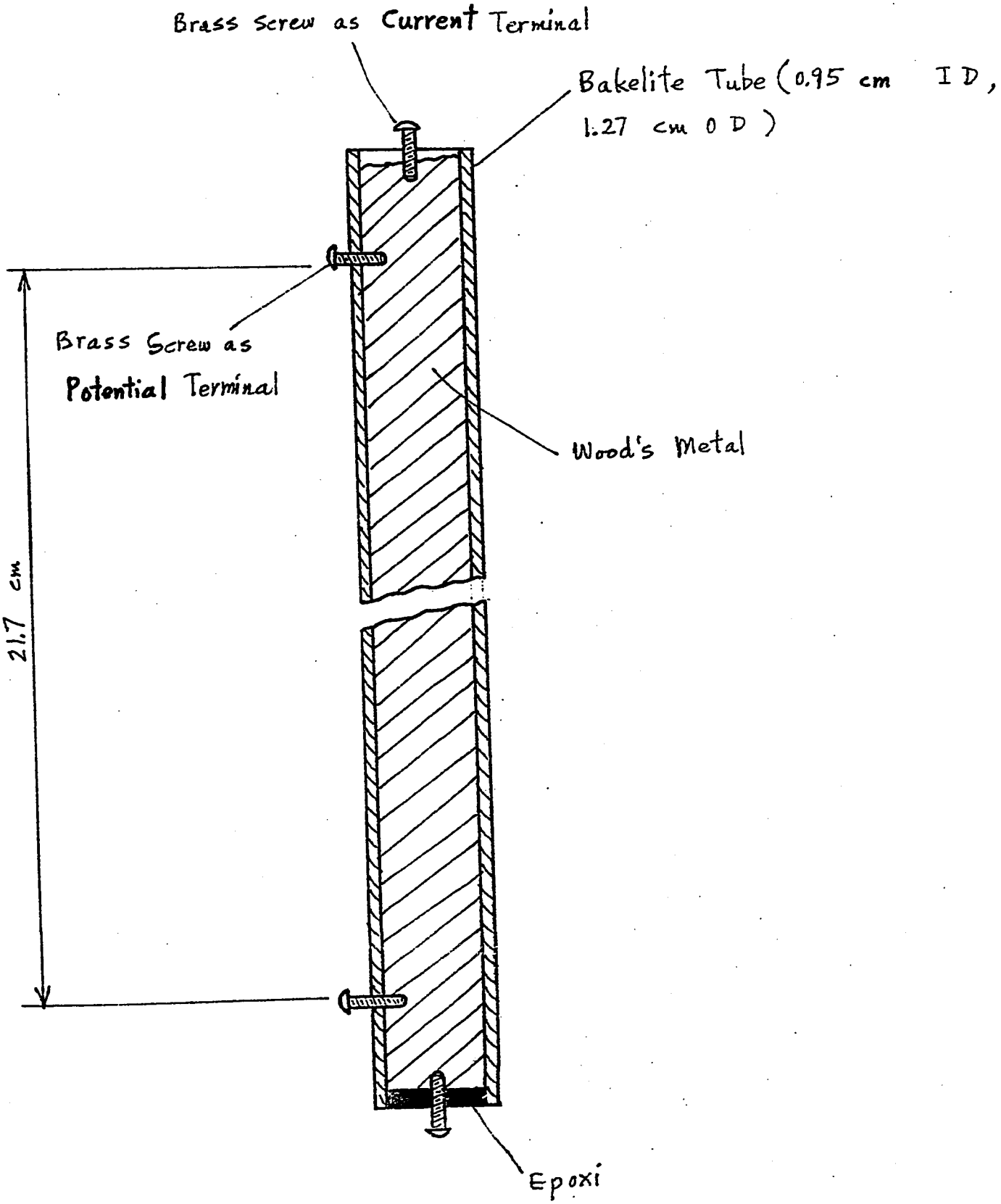

Fig. 31 : Apparatus for measuring Resistivity of Wood's Metal

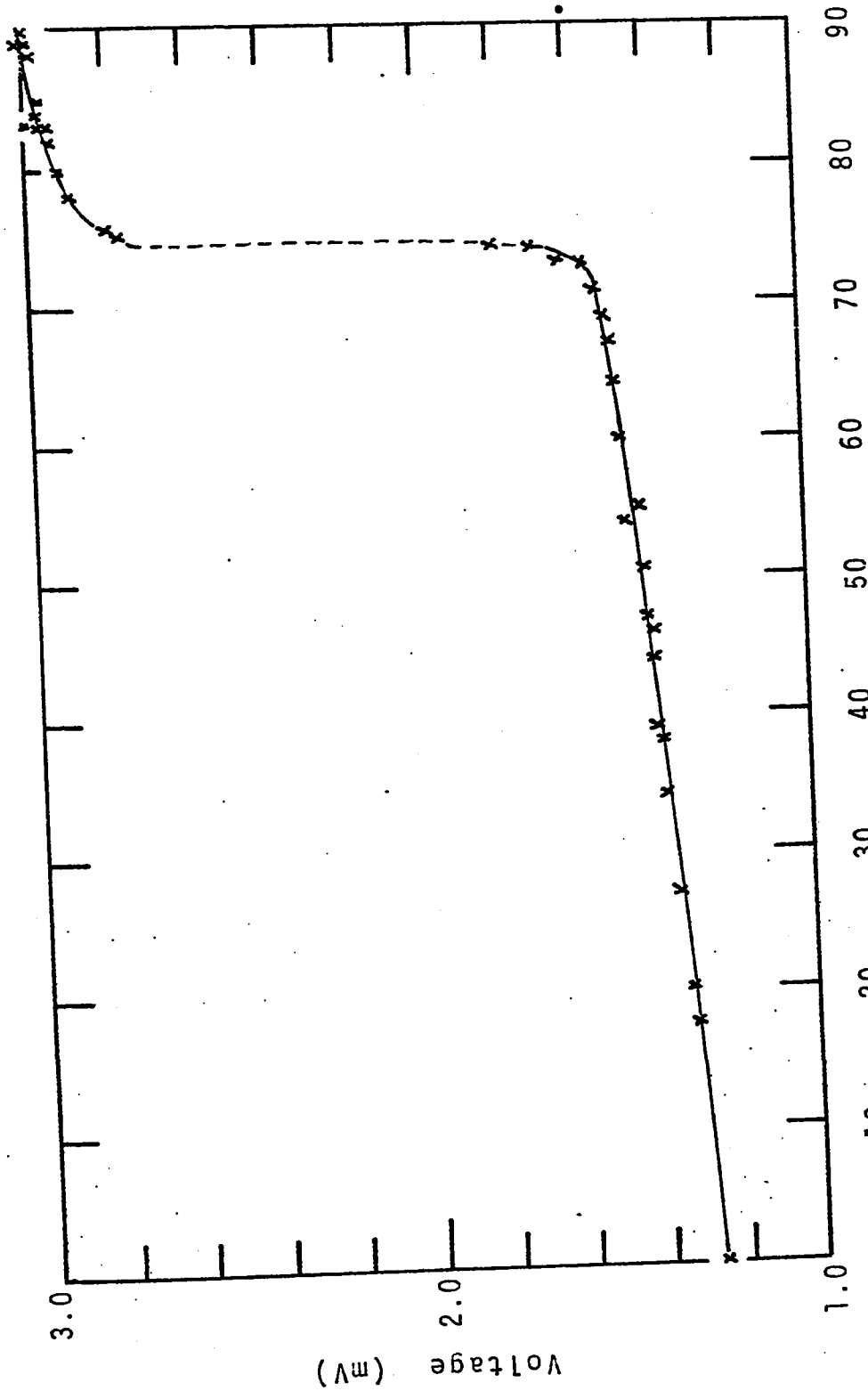

Fig. 32: Voltage-Temperature Characteristic of the Specimen of Wood's Metal

References

1. Phillips, M., "Car pollution-cheap solution," Engineering, vol. 210, no. 5466, pp. 845-855, March 1971.

2. Hoffman, G. A., "The electric automobile," Scientific American, vol. 215, no. 4, pp. 34-40, October 1966.

3. Ross, H. R., "The future of the automobile," Science & Technology, no. 8, pp. 14-24, August 1968.

4. Mooney, J. J., and Blamble, K. W., "Diesel exhaust purification with fixed bed catalyst," Engelhard Industries Technical Bulletin, vol. 9, no. 3, pp. 85-89, December 1968.

5. Millan, J., "Run a car on bottled gas," Engineering, vol. 210, no. 5463, pp.764-765, February 1971.

6. Ludvigsen, K., "Stirling engine," Road & Track, vol. 24, no. 7, pp. 83-91, March 1973.

7. Gottlieb, J. J., "Present status of electric automobiles," National Research Council Report DME/NAE 1970 (4), pp. 3-38, Ottawa, Canada, 1970.

8. Hender, B. S., "Future of the batter-electric car," Electronics & Power, vol. 10, pp. 250-254, August 1964.

9. Lee, M., "Electric vehicles," Science Journal, vol. 3, no. 3, pp. 35-42, March 1967.

10. Rishavy, E. A., Bond, W. D., and Zechin, T. A., "Electrovair--a battery electric car," SAE Paper 670175, January 1967.

11. Marks, C., Rishavy, E. A., and Wyczalek, F. A., "Electrovan--a fuel cell powered vehicle," SAE Paper 670176, January 1967.

12. Miyake, Y., "Electric cars proliferate in Japan," SAE Journal, vol. 77, no. 8, pp.43-47, August 1969.

13. Wheeler, C. M., "Motors for electric vehicles," SAE Paper 690126, January 1969.

14. Agarwal, P. D., and Levy, I. M., "A high performance ac electric drive system," SAE Paper 670178, January 1967.

15. Polgreen, G. R., "The ideal magnet--fully controllable permanent magnets for power and transport," Electronics & Power, vol. 17, pp. 31-34, January 1971.

16. Ramshaw, R. S., and Jani, A. C., "Aspects of a d.c. homopolar servomotor," Direct Current, vol. 10, no. 5, pp. 80-83, May 1965.

17. Danthine, A. A. S., and Pirotte, P. L. R., "Design of shell-type d-c motors for minimum weight," IEEE Trans. on Applications and Industry, vol. 82, pp. 345-351, November 1963.

18. Campbell, P., "A new wheel motor for electric commuter cars," Electrical Review, vol. 190, no. 10, pp. 332-333, March 1972.

19. Morman, W. H. (Jr.), Ramsey, M. H., and Hoft, R. G., "50-kW thyristor dc-to-dc converter," IEEE trans. on Industry Applications, vol. IA-8, no. 5, pp. 617-635, September/October 1972.

20. "Generator successfully combines superconducting windings and liquid-metal contacts," Machine Design, vol. 43, no. 27, p.18, November 1971.

21. Noeggerath, J. E., "Acyclic (homopolar) dynamos," Trans. AIEE, vol. 24, pp. 1-18, January 1905.

22. "Superconducting motor," Electronics & Power, vol. 14, p. 114, March 1968.

23. McNab, I. R., and Wilkin, G. A., "Carbon-fibre brushes for superconducting machines," Electronics & Power, vol. 18, pp. 8-10, January 1972.

24. Marshal, R. A., "Design of brush gear for high current pulses and high rubbing velocities," IEEE Trans. on Power Apparatus and Systems, vol. PAS-85, no. 11, pp. 1177-1187, November 1966.

25. Lewis, D. L., "Homopolar d.c. machines for industry," Electrical Review, vol. 189, no. 4, pp. 119-122, July 1971.

26. Zeisler, F. L., "A high power density electric machine element," IEEE

Trans. on Power Apparatus and Systems, vol. PAS-86, no. 7, pp. 811-818, July 1967.

27. Burnett, J. R., and Kaestle, F. L., "Acyclic generator--a new d.c. power generation tool for industry," Direct Current, vol. 8, no. 7, pp. 196-201, July 1963.
28. Appleton, A. D., "The status of superconducting machines," DE INGENIEUR JRG. 84 NR. 11 A 224-227 MAART 1972.
29. Holm, R., "Electric contacts," 4th ed., Springer-Verlag, New York, 1967, pp. 47-51.
30. "Bibliography and abstracts on electrical contacts, circuit breakers, and arc phenomena, 1965-1969," prepared by Steering Committe of the Holm Seminar on Electric Contact Phenomena, and by Technical Committee of Parts Materials and Packaging Group of IEEE.
31. Holm, R., "Electric contacts handbook," 3rd ed., Springer-Verlay, Berlin, 1958, p. 401 and p. 403.
32. Ref. (29), p. 221
33. Lindenblad, N. E., U. S. Patent 2467758, 1949.
34. Dauphinee, T. M., and Preston-Thomas, H., in "Temperature--its measurement and control in science and industry," vol. 3, pt. 1, Reinhold Publishing Corp., New York, 1962, chapt. 76.
35. Dauphinee, T. M., "Some applications of dc and square wave ac techniques to undersea measurements," ISA Paper 68-635, October 1968.
36. Ref. (29), p. 1.
37. "Carbon brushes and electrical machines," Morganite Carbon Ltd., London, 1961, p. 24.
38. Ref. (29), p.368.
39. Roark, R. J., "Formulas for stress and strain," 3rd ed., McGraw-Hill, New York, 1954, p.287.

40. Hodgman, C. D., "Handbook of chemistry and physics," 32nd ed., Chemical Rubber Publishing Co., Cleveland, 1950, p. 1802.

41. Hague, B., "The principles of electromagnetism applied to electrical machines," Dover, New York, 1962, pp. 345-350.

42. Dwight, H. B., "Two cases of calculation of mechanical forces in electric circuits," J. AIEE, pp. 1238-1240, November 1927.

43. Ref. (40), p. 1799.

44. Ref. (29), pp. 60-64.

45. Llewellyn-Jones, F., "The physics of electrical contacts," Oxford University Press, London, 1957, pp. 17-20.

46. Ref. (40), pp. 1344-1347.

47. Ref. (29), pp. 443-476.

48. Ref. (41), pp. 146-149.

49. Bron, O. B., Elektrotekhnika, vol. 36, no. 1, 1965, pp. 21-23; "The electrodynamic forces on contacts," Soviet Electrical Engineering, vol. 36, no. 1, pp. 33-37, January 1965.

50. Whitelaw, R. L., "Fighting automobile air pollution: the hydrostatic drive and the flywheel-electric LDV," Engineering Digest, vol. 19, no. 2, pp. 27-31, February 1973.

VITA

Name:	Che Keung Ma
Born	Canton, China, November 3. 1937.
Education:	
Secondary:	New Method College, Hong Kong.
Tech. College:	Hong Kong Technical College, Hong Kong.
University:	McGill University, B. Eng. in Electrical Engineering, 1964.

UNIVERSITE D'OTTAWA / UNIVERSITY OF OTTAWA
École des études supérieures/School of Graduate Studies

Title of thesis LIQUID-METAL-WETTED ROLLING-CONTACT CURRENT COLLECTORS

Name of candidate MA, Che-Keung

Degree M.A.Sc. Department Electrical Engineering

Date of defence May 25th, 1973

We, the undersigned, certify that we have approved this thesis and that the candidate has defended it successfully.

J.V. Marsh J. V. Marsh
(Signature of Examiners)

K. Schenk K. F. Schenk

O. Celinski O. Celinski
(Thesis Supervisor)

Paul Hogen
(Dean of Graduate Studies)

UNIVERSITÉ D'OTTAWA / UNIVERSITY OF OTTAWA
École des études supérieures/School of Graduate Studies

NAME OF AUTHOR MA, Che-Keung

TITLE OF THESIS LIQUID-METAL-WETTED ROLLING-CONTACT CURRENT COLLECTORS

DEGREE Master of Applied Science (Electrical Engineering) YEAR GRANTED 1973

Che Keung Ma
(Signed) (Author)

Date: May 25th, 1973

Permanent Address:
Box 425, RR 2, Greely,
Ontario, K0A 1Z0